Journal of Paleontology, 92(2), 2018, p. 272–288

0022-3360/18/0088-0906
doi: 10.1017/jpa.2017.62

JOURNAL OF PALEONTOLOGY
A PUBLICATION OF THE Paleontological SOCIETY

New material and systematic re-evaluation of *Medusaceratops lokii* (Dinosauria, Ceratopsidae) from the Judith River Formation (Campanian, Montana)

Kentaro Chiba,[1] Michael J. Ryan,[2] Federico Fanti,[3,4] Mark A. Loewen,[5,6] and David C. Evans[1,7]

[1]Department of Ecology and Evolutionary Biology, University of Toronto, 25 Willcocks Street, Toronto, Ontario, M5S 3B2, Canada ⟨kentaro.chiba@mail.utoronto.ca⟩
[2]Department of Vertebrate Paleontology, Cleveland Museum of Natural History, 1 Wade Oval Dr., University Circle, Cleveland, Ohio, 44106, USA ⟨mryan@cmnh.org⟩
[3]Dipartimento di Scienze Biologiche, Geologiche e Ambientali, Alma Mater Studiorum, Università di Bologna, Via Zamboni, 67 - 40126 Bologna, Italy ⟨federico.fanti@unibo.it⟩
[4]Museo Geologico Giovanni Capellini, Via Zamboni, 63 - 40126 Bologna, Italy
[5]Department of Geology and Geophysics, University of Utah, Salt Lake City, Utah, 84112-0102, USA
[6]Natural History Museum of Utah, Salt Lake City, Utah, 84108, USA ⟨mloewen@umnh.utah.edu⟩
[7]Royal Ontario Museum, 100 Queen's Park, Toronto, Ontario, M5S 2C6, Canada ⟨d.evans@utoronto.ca⟩

Abstract.—*Medusaceratops lokii* Ryan, Russell, and Hartman, 2010 is an enigmatic taxon of ceratopsid represented by partial parietals from the Mansfield bonebed in the Campanian Judith River Formation, Montana. Originally, all ceratopsid material collected from this bonebed was referred to the centrosaurine ceratopsid *Albertaceratops*, but subsequently two parietals were designated the types of the chasmosaurine, *M. lokii*, in part, because they were interpreted to have three epiparietals bilaterally. Here we describe new material from the bonebed that allows a systematic revision of the taxon. A revised reconstruction of the frill, informed by newly discovered parietals, reveals that *M. lokii* had a broad midline ramus and at least five epiparietals (ep) around the margin of the frill, both traits that are characteristic of Centrosaurinae. From medial to lateral, the epiparietal ornamentation consists of a small, variably procurving epiparietal (ep 1), an anterolaterally curving pachyostotic hook (ep 2), a smaller pachyostoic process (ep 3), and two small triangular epiparietals (ep 4 and 5). A phylogenetic analysis of ceratopsids, which is the first to include *Medusaceratops*, indicates that *M. lokii* is a unique, early centrosaurine ceratopsid taxon that is more closely related to Centrosaurini and Pachyrhinosaurini than Nasutoceratopsini. No unequivocal chasmosaurine bones or diagnostic material from any other ceratopsid could be identified from the Mansfield bonebed, suggesting that it represents one of the oldest occurrences of a monodominant accumulation of a centrosaurine ceratopsid on record.

Introduction

Ceratopsids are a clade of large-bodied herbivorous dinosaurs that rapidly diversified in the latest Cretaceous (Campanian–Maastrichtian) of North America, and have a well-sampled fossil record (Dodson et al., 2004). Recent discoveries from southern Alberta (Ryan, 2007; Ryan et al., 2010, 2012; Evans and Ryan, 2015), Montana (Longrich, 2013; Ryan et al., 2014), and Utah (Loewen et al., 2013; Sampson et al., 2013; Lund et al., 2016a) have revealed a diversity of early ceratopsids that have significantly increased our knowledge of the plesiomorphic anatomy of the group. However, the fossil record of the early radiation of ceratopsids remains poor, and in light of new anatomical information that obscures the morphological distinction between the two subfamilies, Centrosaurinae and Chasmosaurinae, conventional wisdom about the systematic position of taxa known from fragmentary material may require re-evaluation (Mallon et al., 2016).

Medusaceratops lokii Ryan, Russell, and Hartman, 2010 from the lowermost strata of the Judith River Formation is one such ceratopsid taxon that has a complicated taxonomic history, with the hypodigm having been previously assigned to both subfamilies. The material of the taxon was collected from a middle Campanian bonebed, called the Mansfield bonebed (ca. 79 Ma; Roberts et al., 2013), making it one of the oldest known members of Ceratopsidae (Kirkland and DeBlieux, 2010; Longrich, 2013; Evans and Ryan, 2015; Campbell et al., 2016). The Mansfield bonebed ceratopsid material was initially assigned to *Albertaceratops nesmoi* Ryan, 2007, which is unequivocally a basal member of Centrosaurinae, based on superficial resemblances of some morphologies to the *A. nesmoi* holotype, such as the large supraorbital horncores and the large pachyostotic parietal hook (Ryan, 2007). Subsequently, the two most complete parietals from the bonebed were described as a new chasmosaurine species, *Medusaceratops lokii,* based on an interpretation of the specimens exhibiting only three epiparietals on each side of the midline, which is typical of Chasmosaurinae (Ryan et al., 2010). The remaining material from the bonebed was left as indeterminate Centrosaurinae (Ryan et al., 2010).

However, Longrich (2013) retained the original centrosaurine designation, noting that the number of epiparietals is variable in Chasmosaurinae, and the parietosquamosal contact more closely resembles that of Centrosaurinae.

Here, we describe newly collected centrosaurine material from the Mansfield bonebed, re-examine the type series of *Medusaceratops*, reassess the known specimens from the bonebed, and conduct a systematic revision of the taxon. New data allow *Medusaceratops* to be included in a numerical cladistic analysis for the first time. We confirm the subfamilial identity of *Medusaceratops* as an early centrosaurine, which has implications for understanding the early diversification of ceratopsids.

Geological context

The Mansfield bonebed is located in the badlands of Kennedy Coulee, north of Rudyard, Hill County, Montana, USA (Fig. 1.1). Here, the middle Campanian alluvial deposits, commonly referred to the lower Judith River Formation (Goodwin and Deino, 1989), crop out extensively along the drainage systems flowing toward the Milk River Valley in the north (Fig. 1.2, 1.3). Following recent stratigraphic revision of the Judith River Formation by Rogers et al. (2016), the beds exposed at Kennedy Coulee correlate to the McClelland Ferry Member to the south, but also with the upper Foremost and overlying lower Oldman formations of southern Alberta to the north, including the Taber Coal Zone (TCZ) and the Herronton Sandstone Zone (HSZ; Ogunyomi and Hills, 1977; Eberth and Hamblin, 1993; Cullen et al., 2016). The TCZ, which represents the top of the Foremost Formation in Alberta and correlative coal deposits exposed to the south, represents a datum for calibrating stratigraphic sections and associated fossil taxa (Eberth and Hamblin, 1993; Brinkman et al., 2004; Ryan, 2007; Evans and Ryan, 2015; Freedman Fowler and Horner, 2015; Cullen et al., 2016; Ryan et al., 2017). The Mansfield bonebed occurs ~10 m above the top of the Marker A Coal layer, which is equivalent to the top of the TCZ (sensu Goodwin and Deino, 1989) based on multiple sections measured in the Kennedy Coulee and at the *Probrachylophosaurus bergei* Freedman, Fowler, and Horner, 2015 locality (MOR locality JR-518), which is ~8 km to the north east. There are two bentonite layers occurring ~10 m below and ~25 m above the TCZ, which provides radiometric ages of 79.02 and 78.01 Ma, respectively (Roberts et al., 2013, but see Freedman Fowler and Horner, 2015 and Fowler, 2016 for discussion), that bracket the Mansfield bonebed and constrain its chronostratigraphic age. The bonebed host beds sit on top of a 10 m thick interval of interbedded organic-rich mudstones with discontinuous carbonaceous seams, siltstone, and sandstones (Fig. 1.4). Fossils occur at the base of a 3 m thick, fining-upward sandy channel deposit that is rich in ironstone nodules; paleocurrent measurements suggest predominant flows toward the ESE.

The stratigraphic occurrence of *Medusaceratops* places the taxon above the Herronton Sandstone Zone in the same stratigraphic interval where *Albertaceratops* and *Wendiceratops* were recovered ~25 km to the northwest in southern Alberta. Correlation to the top of the TCZ places *Albertaceratops* slightly lower in the section (8 m above the TCZ) with respect to *Medusaceratops* (10 m above the TCZ) and *Wendiceratops* (12 m above the TCZ), making them virtually indistinguishable stratigraphically. Due to the discontinuous nature of the beds

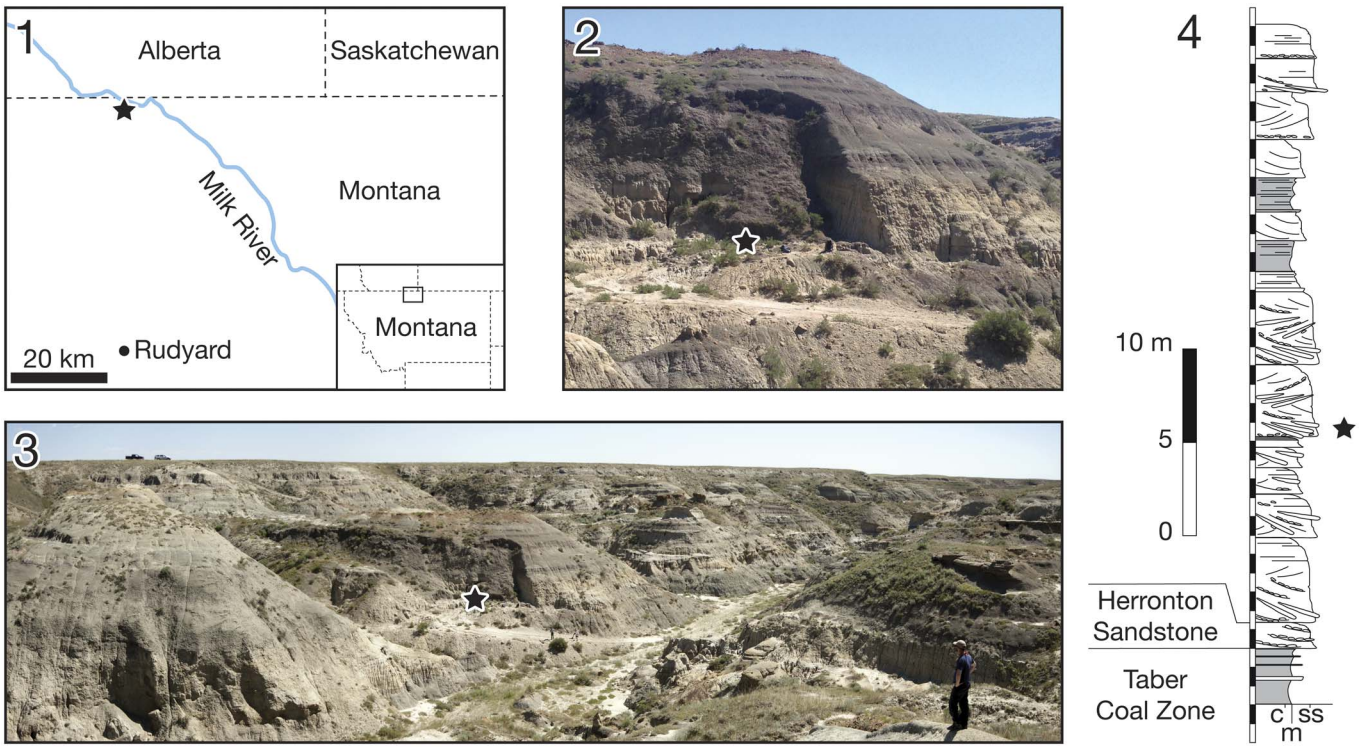

Figure 1. (**1**) Locality map of the Mansfield bonebed. (**2, 3**) Overview photos of the locality area. (**4**) Stratigraphic column of the locality area. The bonebed is indicated by a black star.

https://doi.org/10.1017/jpa.2017.62 Published online by Cambridge University Press

forming the HSZ and the channelized deposits in which the *Medusaceratops* bonebed occurs, the reciprocal occurrence of these taxa may be slightly inaccurate.

Materials and methods

The Mansfield bonebed has been commercially excavated by Canada Fossils Ltd since 1994. The bonebed specimens previously described in Ryan (2007) and Ryan et al. (2010) are housed in the Royal Tyrrell Museum of Palaeontology (TMP) and the Wyoming Dinosaur Center (WDC). The new material described here was collected in the summer of 2011 and 2012 by a crew led by D. Trexler of the Two Medicine Dinosaur Center in Bynum, Montana, and subsequently acquired by the Royal Ontario Museum. The quarry was visited by DCE and FF on July 16, 2016, where a detailed stratigraphic section was measured and sedimentological observations were made at the quarry site.

Photogrammetric 3D models of selected specimens (Figs. 3, 6) were created using Agisoft PhotoScan Standard Edition, ver. 1.1 and 1.2 to help visualize certain morphologies that can be obscured by the dark color of the specimens. The models were exported as STL files and scaled to the original size in mm using MeshLab, ver. 1.3.3 (SourceForge). The models were then oriented and screen-captured on Avizo, ver. 6.1.1. (FEI). The 3D models were uploaded to Dryad (http://doi.org/10.5061/dryad.8h067).

For the phylogenetic analysis, *Medusaceratops* was coded into the data matrix of Ryan et al. (2017) based on the hypodigm listed in the supplemental material (Text S1 and Table S1). Based on our interpretation of the available material, there is no indication of any other ceratopsid species in the Mansfield bonebed collections, and it is therefore assumed to be a monodominant bonebed, which is common for centrosaurines (Ryan et al., 2001; Eberth and Getty, 2005; Ralrick and Tanke, 2008; Chiba et al., 2015; Eberth, 2015). Hence, all ceratopsid material from the bonebed is interpreted to represent a single species, and coded as a single operational taxonomic unit, following common practice in centrosaurine studies (e.g., Sampson et al., 1995; Ryan and Russell, 2005; Currie et al., 2008; Farke et al., 2011; Fiorillo and Tykoski, 2012; Ryan et al., 2012; Evans and Ryan, 2015). We added *Medusaceratops lokii* and the recently described centrosaurine, *Machairoceratops cronusi* Lund et al., 2016a into the original data matrix, which includes 28 ceratopsian operational taxonomic units.

The final matrix is composed of 101 characters, which includes 97 characters used first in Farke et al. (2011) and subsequently used in Sampson et al. (2013), and four characters added by Evans and Ryan (2015). All characters were equally weighted, but Character 20 was treated as an ordered (additive) character following previous analyses (e.g., Farke et al., 2011; Sampson et al., 2013; Evans and Ryan, 2015). Codings of two characters are modified from Ryan et al. (2017). Reassignment of the Mansfield bonebed material to *Medusaceratops* in this paper results in the coding change for Character 30 (curvature of supraorbital horncore in rostral view) for *Albertaceratops* from '2' (lateral) to '?'. Character 100 (shape of epiparietal 1) was modified for two taxa as follows: from 1 to 2 (elongate flattened process or spike, greater than twice as long as wide) in *Coronosaurus brinkmani* (Ryan and Russell, 2005) based on TMP 2002.068.0001; from 1 to (0 and 1) in *Styracosaurus albertensis* Lambe, 1913 reflecting polymorphism based on CMN 344 and ROM 1436 (Ryan et al., 2007). We follow the epiparietal homology argument of Evans and Ryan (2015), which counts the most medially positioned paired epiparietals as ep 1 in non-eucentrosauran (see following paragraph) centrosaurines. The phylogenetic analysis was performed using Traditional Search with the Tree Bisection Reconnection algorithm in TNT ver. 1.5 (Goloboff and Catalano, 2016) with *Leptoceratops gracilis* Brown, 1914b designated as the outgroup taxon, following the previous analysis (Sampson et al., 2013). The analysis was run with 1,000 replicates, and up to 1,000 trees were saved in each replication. Branches are collapsed if there is no possible support ("Rule 3"). To assess the robustness of the attained topology, standard bootstrap resampling (sampling with replacement) was conducted with 10,000 replications of traditional tree search, and Bremer support was computed with retaining trees suboptimal by ten steps. In order to further test the subfamilial phylogenetic position of *Medusaceratops lokii* as a centrosaurine rather than a chasmosaurine, a constraint analysis was performed in which the position of *M. lokii* was constrained as the sister taxon of *Chasmosaurus* and *Pentaceratops* in a monophyletic Chasmosaurinae, using this option in TNT.

We define the new node-based centrosaurine clade Eucentrosaura as the least inclusive clade containing *Centrosaurus apertus* and *Pachyrhinosaurus canadensis* in order to facilitate the morphological comparisons of the *Medusaceratops* material with other centrosaurines in this study. Eucentrosaura includes the members of Centrosaurini and Pachyrhinosaurini recovered in the strict consensus tree topology described in the phylogenetic analysis section of this paper, which is consistent with other recent phylogenetic analyses of centrosaurines (e.g., Farke et al., 2011; Evans and Ryan, 2015; Ryan et al., 2017).

A histological thin section of the diaphysis of a large tibia (ROM 67873) was made using standard techniques (Lamm, 2013) in the palaeohistology lab at the Royal Ontario Museum. The original thin section images made using plane and cross-polarized light are available at http://doi.org/10.5061/dryad.8h067.

Repositories and institutional abbreviations.—Canadian Museum of Nature (CMN), Ottawa, Canada; Fukui Prefectural Dinosaur Museum (FPDM), Fukui, Japan; Museum of the Rockies (MOR), Bozeman, Montana, USA; Royal Ontario Museum (ROM), Toronto, Ontario, Canada; Royal Tyrrell Museum of Palaeontology (TMP), Drumheller, Alberta, Canada; Wyoming Dinosaur Center (WDC), Thermopolis, Wyoming, USA.

Systematic paleontology

Dinosauria Owen, 1842
Ornithischia Seeley, 1887
Ceratopsia Marsh, 1890
Neoceratopsia Sereno, 1986
Ceratopsidae Marsh, 1888
Centrosaurinae Lambe, 1915
Medusaceratops Ryan, Russell, and Hartman, 2010

Medusaceratops lokii Ryan, Russell, and Hartman, 2010

https://doi.org/10.1017/jpa.2017.62 Published online by Cambridge University Press

Holotype.—WDC-DJR-001, an incomplete parietal comprised of a largely complete left lateral bar with loci for epiparietals (ep) 1–5 (Fig. 2.1–2.4).

Paratype.—WDC-DJR-002, a right partial parietal with ep 1–3 (Fig. 2.5, 2.6).

Referred material.—All centrosaurine ceratopsid material from the Mansfield bonebed. See supplementary table (Table S1) for the complete list of the referred material examined in this paper.

Locality and horizon.—The Mansfield bonebed is located in the outcrop along the Kennedy Coulee near Rudyard, Montana, USA (Fig. 1.1). Detailed locality data is on file at the ROM, TMP, and WDC. The bonebed layer is located ~10 m above the top of the Marker A coal (Goodwin and Deino, 1989) in the McClelland Ferry Member of the Judith River Formation (Rogers et al., 2016). The age of the bonebed is constrained between 79.0 Ma and 78.7 Ma by radiometric dates derived from bentonites that occur 5 m below and 27 m above the top of the Marker A Coal, respectively, within Kennedy Coulee (Roberts et al., 2013, but see

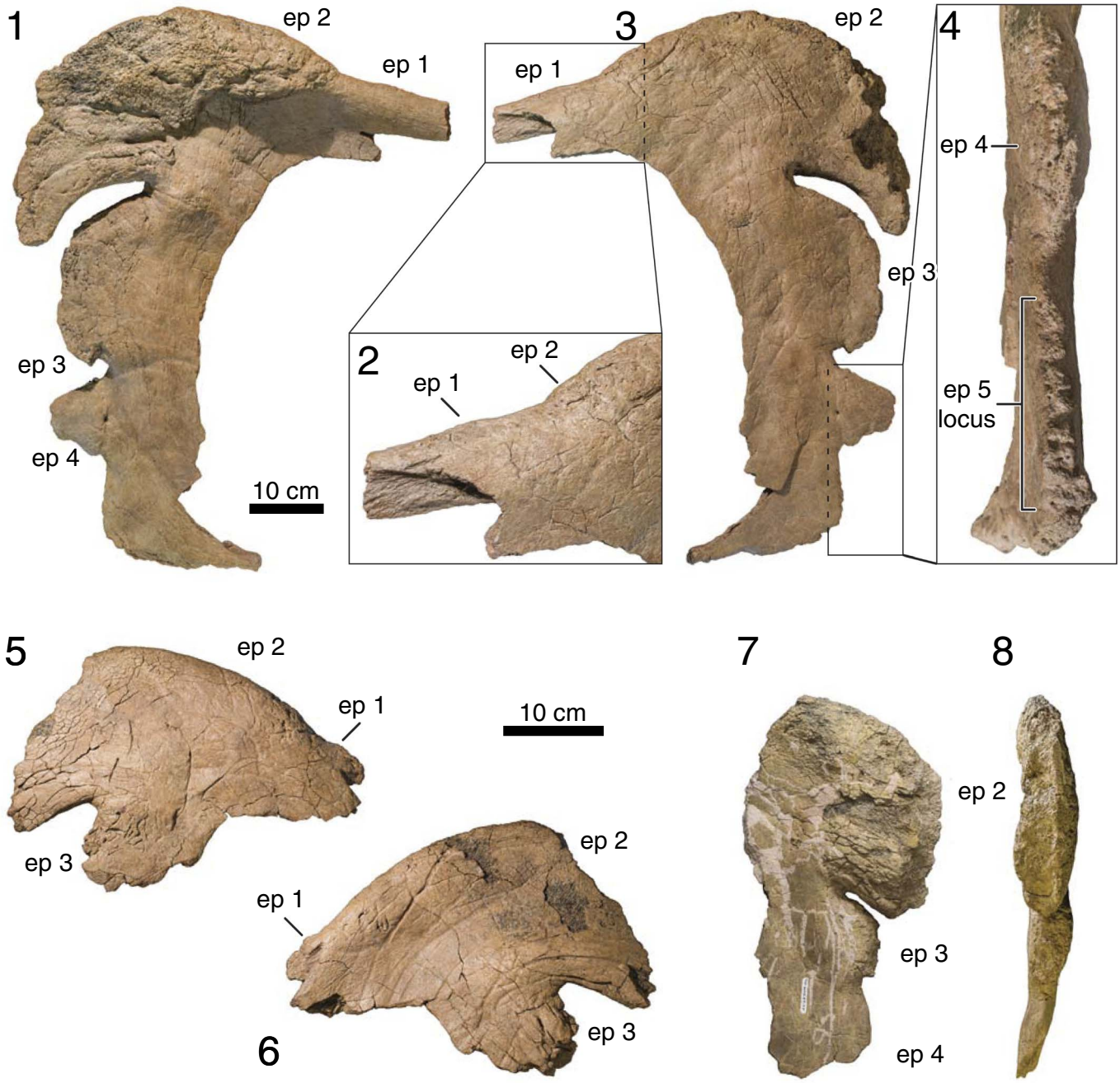

Figure 2. Previously described parietals from the Mansfield bonebed: (**1**) ventral view, (**2**) close-up of ep 1, (**3**) dorsal view, and (**4**) close-up of lateral view of lateral ramus of WDC-DJR-001; (**5**) dorsal and (**6**) ventral views of WDC-DJR-002; (**7**) ventral and (**8**) lateral view of TMP 2002.069.0005. Upper and lower scale bars are for (**1, 3**) and (**5–8**), respectively. Abbreviation: ep, epiparietal.

https://doi.org/10.1017/jpa.2017.62 Published online by Cambridge University Press

Freedman Fowler and Horner, 2015 and Fowler, 2016 for discussion).

Emended diagnosis.—Centrosaurine ceratopsid with five epiparietals on posterolateral parietal ramus, from medial to lateral: ep 1, a small, sometimes procurved epiparietal; ep 2, comparatively massive, broad-based pachyostotic process that is strongly curved and projects anterolaterally; ep 3, small pachyostotic process curved anterolaterally, with a similar shape to ep 2; ep 4 and ep 5, unmodified, small triangular-shaped epiparietals. *Medusaceratops* differs from *Albertaceratops* in possession of a low, elongate ep 1 as the medialmost epiparietal, and differs from *Xenoceratops* in the strong anterior curvature and projection of ep 2.

Remarks.—The specimen figured as the paratype in the original description of *Medusaceratops* (Fig. 12.2 in Ryan et al., 2010) is not WDC-DJR-002, but TMP 2002.069.0005. Here, we retain WDC-DJR-002 as a paratype since this specimen preserves the diagnostic combination of parietal ornamentation, notably part of the small ep 1 and the pachyostotic ep 2, rather than TMP 2002.069.0005. Casts of the holotype and paratype specimens are reposited at the ROM and at the TMP.

WDCB-MC-001, is a large, intact region of the skull roof that includes nasal and postorbital ornamentation, that was reported to have been collected from the Mansfield bonebed by Ryan (2007). However, new information suggests that, although it was collected in Kennedy Coulee, it probably did not originate in the bonebed (D. Trexler, personal communication, 2017). For this reason, and the fact that the postorbital horncores are much shorter than any known from the bonebed, we do not include it in the hypodigm of *Medusaceratops lokii* at this time.

Description

The frill ornamentation, composed of co-ossified episossifications, and the facial horns are generally the most diagnostic suite of traits for ceratopsid dinosaurs, especially for centrosaurines (Dodson et al., 2004), thus we describe only the parietal, squamosal, postorbital, and nasal below, following previous work (e.g., Ryan and Russell, 2005). Due to the incomplete nature of the material, and to provide clarity with respect to the new interpretations presented here, detailed descriptions of individual specimens are provided in the appropriate sections, following a general description of each element. A comprehensive list of specimens comprising the hypodigm of *Medusaceratops* referred to in this study is provided in the supplemental data (Table S1).

Parietal.—Re-examination of WDC-DJR-001 (holotype; Fig. 2.1–2.4), with reference to ROM 73832 (Fig. 3.1–3.5) and ROM 73836 (Fig. 3.8–3.10) indicates that *Medusaceratops lokii* has five, not three, epiparietals (Fig. 4.3). These are the newly recognized diminutive epiparietal (ep 1) and the small triangular-shaped epiparietal (ep 5) that are positioned medially and laterally, respectively, to the three epiparietals that were originally recognized by Ryan et al. (2010). From medial to lateral, these epiparietals have the following morphology: one small epiparietal (ep 1) sits on the posterior margin of the posterior ramus adjacent to the midline (i.e., ROM 73832, ROM 73837, WDC-DJR-001, and WDC-DJR-002); a large pachyostotic hook (ep 2) curves anterolaterally (i.e., WDC-DJR-001, WDC-DJR-002, and TMP 2002.069.0005), a smaller pachyostotic hook (ep 3) curves subtly anterolaterally (i.e., WDC-DJR-001, TMP 2002.069.0005), and two smaller, triangular-shaped epiparietals (ep 4 and 5; i.e., ROM 73836 and WDC-DJR-001).

The number of parietal processes of *Medusaceratops* and other morphological features seen on parietals from the bonebed do not reveal any definitive chasmosaurine traits. However, they exhibit several key centrosaurine characters, such as a broad midline ramus (ROM 73832), imbricated epiparietals (ROM 73836; also seen on the previously described holotype WDC-DJR-001, as well as TMP 2002.069.0005), and a convex, interdigitating squamosal contact (ROM 73836) (Longrich, 2013). Longrich (2013) noted that the preserved epiparietals are different between WDC-DJR-001 and TMP 2002.069.0005 due to the size discrepancies of ep 3 (P2 in Ryan et al., 2010). However, the ep 3 of TMP 2002.069.0005 is lobe-shaped rather than being an unmodified, triangular shape. Therefore, we agree with the interpretation of Ryan et al. (2010) that the preserved epiparietals on TMP 2002.069.0005 are ep 2–4. We interpret the size difference of ep 3 on TMP 2002.069.0005 and WDC-DJR-001 as an individual and/or ontogenetic variation.

ROM 73832 (Fig. 3.1–3.5).—ROM 73832 preserves the posterior half of a midline ramus and the medial part of the left posterior ramus with a distinct yet diminutive epiparietal (ep 1) adjacent to the midline. The ventral surface is relatively smooth, whereas the dorsal side is incised by numerous vascular grooves, especially on the tori on the midline ramus and the epiparietal on the posterior ramus, and has adult bone texture (sensu Sampson et al., 1997; Brown et al., 2009). Ep1 is well fused to the posterior ramus, and its contact boundary is indistinguishable (Fig. 3.3). Taken together, the bone surface texture, the epiparietal fusion, and the thickened posterior margin of the midline ramus (31.6 mm), suggest that this specimen is derived from a skeletally mature, adult individual (Sampson et al., 1997). In cross-section, the midline ramus tapers laterally on either side of the midline, making it transversely broad with a triangular cross-sectional shape (Fig. 3.4), which is a synapomorphy for Centrosaurinae (Farke et al., 2011; Sampson et al., 2013; Evans and Ryan, 2015). The midline ramus has two low tori ('bumps') on the dorsal side (Fig. 3.1 and 3.5). An embayment of the posterior ramus at the midline is present, but it is wide and relatively shallow (Fig. 3.3), as in *Xenoceratops* (Ryan et al., 2012).

Ep 0 is definitively absent in this specimen. The base of the preserved epiparietal, ep 1, is unusual compared to other

Figure 3. Newly described parietals from the Mansfield bonebed: (**1**) oblique view (direction is figured by arrows above) of 3D model, (**2**) posterior view, (**3**) dorsal view, (**4**) anterior view, and (**5**) left lateral view of ROM 73832; (**6**) dorsal and (**7**) oblique view (direction figured by arrows above) of 3D model of ROM 73837; (**8**) lateral view, (**9**) dorsal view, and (**10**) close-up of ventral surface of ROM 73836. Abbreviations: ep, epiparietal; mb, bumps on midline ramus; mr, midline ramus; pr, posterior ramus; sqc, squamosal contact.

https://doi.org/10.1017/jpa.2017.62 Published online by Cambridge University Press

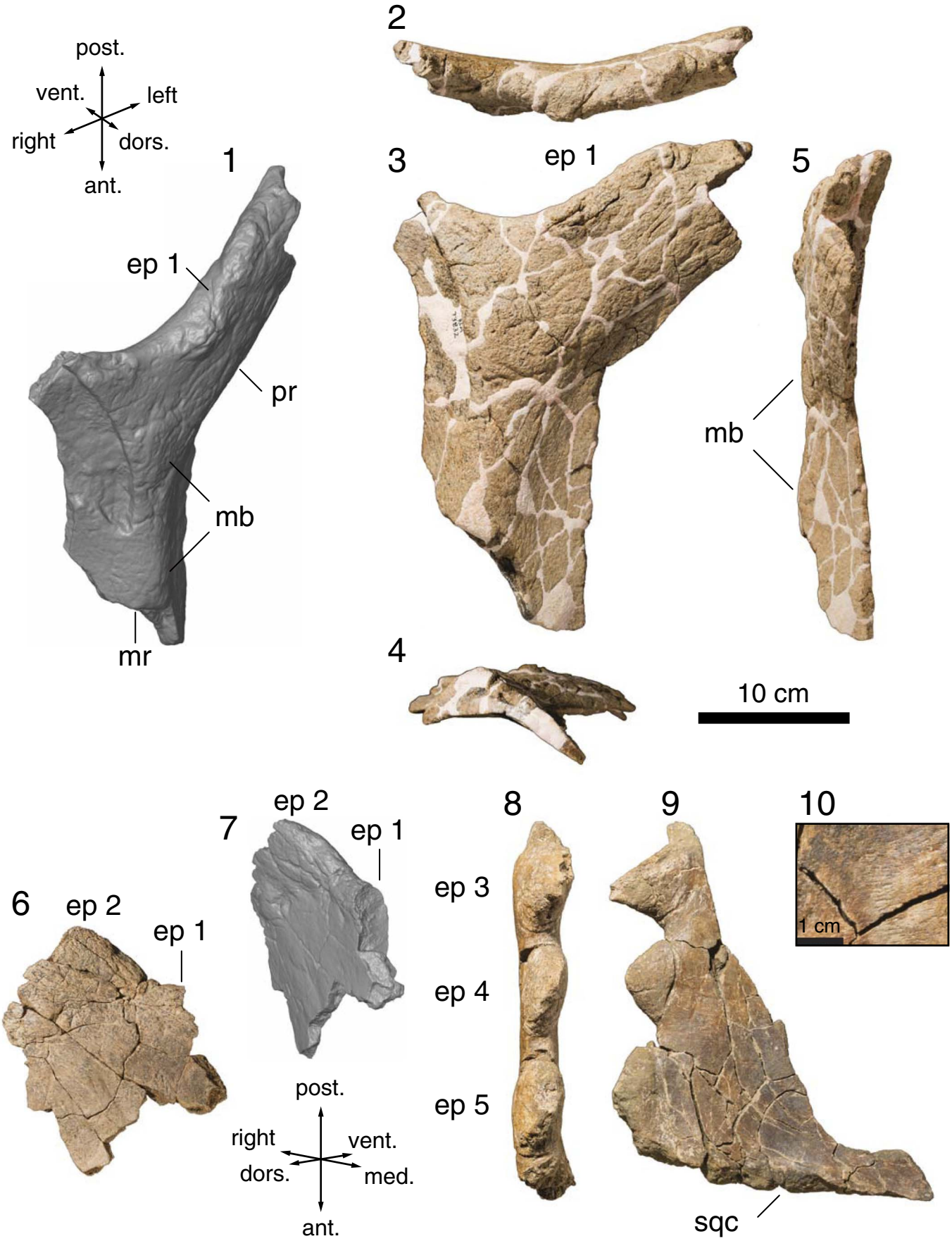

https://doi.org/10.1017/jpa.2017.62 Published online by Cambridge University Press

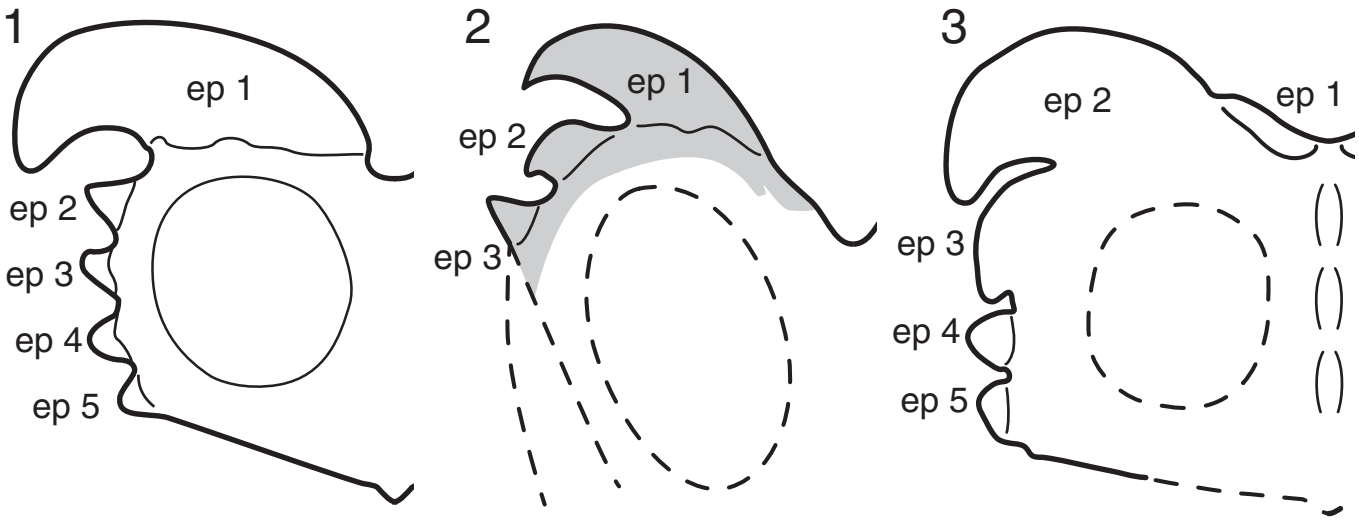

Figure 4. Comparison of frill ornamentations of (**1**) *Albertaceratops nesmoi* in Ryan (2007), (**2**) previous reconstruction of *Medusaceratops lokii* frill in Ryan et al. (2010) (gray part represents where the holotype [WDC-DJR-001] corresponds), and (**3**) new reconstruction of *M. lokii* frill in this study, mainly based on ROM 73832, ROM 73836, and WDC-DJR-001. Abbreviation: ep, epiparietal.

centrosaurines in that the body exhibits a slight torsion such that its medial portion is located on the dorsal surface of the posterior ramus, but the lateral portion is on the posterior margin (Fig. 3.1–3.3). This epiparietal is proportionally broad and low (114.2 by 15.7 mm), but projects forward (Fig. 3.1). Although smaller, it is most similar in morphology and position to the ep 1 of *Xenoceratops foremostensis* Ryan, Evans, and Shepherd, 2012 (P2 in Ryan et al., 2012) among known centrosaurines.

ROM 73836 (Fig. 3.8–3.10).—ROM 73836 is an antero-lateral segment of the parietal that includes the three lateralmost epiparietals (ep 3–5, also see description of WDC-DJR-001 below) and the squamosal contact of the right lateral ramus. Although all three epiparietals are completely fused, the boundary between the epiparietals and the underlying parietal ramus is clearly delineated (Fig. 3.9). On both dorsal and ventral surfaces, the specimen exhibits the combination of a long-grained texture on the lateral side and adult bone texture on the medial side of the lateral parietal ramus (Fig. 3.10). Note that the long-grained texture is always proximally associated with the mottled texture but not the adult texture in centrosaurines (e.g., *Avaceratops*, "*Brachyceratops*," "*Monoclonius*," *Coronosaurus brinkmani*, *Centrosaurus*, *Styracosaurus*, *Pachyrhinosaurus*) that were examined by Brown et al. (2009). The intriguing mixture of textures on ROM 73836 may suggest a unique ontogenetic textual transition in *Medusaceratops*. The squamosal contact is rugose and convex, which is typical of centrosaurines but not known in chasmosaurines (Dodson et al., 2004).

The two epiparietals closest to the squamosal contact (ep 4 and 5) have a low and rounded triangular morphology when viewed dorsally, similar to unmodified epiparietals in other centrosaurines. Comparatively, the epiparietal (ep 3) posterior to these has a shorter base and a tall, triangular profile with an acute apex (Fig. 3.9). Ep 3 closely resembles the morphology and proportions of the lateral epiparietals on the holotype of *Albertaceratops* (TMP 2001.026.0001). All of the epiparietals on ROM 73836 are strongly imbricated (Fig. 3.8), and the squamosal contact is convex, both of which support a centrosaurine assignment for the Mansfield bonebed material (Dodson et al., 2004).

WDC-DJR-001 (holotype, Fig. 2.1–2.4).—Part of the posterior ramus and all of the lateral ramus of the parietal are preserved on WDC-DJR-001, the holotype of *M. lokii*. Long-grained bone texture occurs on the lateral side of the lateral ramus, as seen on ROM 73836. The posterior ramus thickness (28.1 mm) is also similar to that of ROM 73832, the midline bar. Ryan et al. (2010) recognized only three epiparietals on this specimen: from medial to lateral these are; a large, wide-based, and pachyostotic hook; a smaller lobe-shaped process; and a round triangular-shaped epiparietal (Ryan et al., 2010). However, comparisons to ROM 73832 and ROM 73836 suggest that WDC-DJR-001 actually possesses two previously unidentified epiparietal loci, for a total of five.

The additional epiparietals include a diminutive epiparietal medial to the large pachyostotic hook, which we interpret as ep 1, and an open sutural locus for ep 5. The medialmost epiparietal (ep 1) is represented by a small eminence with a porous texture on the posterodorsal margin of the posterior ramus (Fig. 2.2, 2.3). Although the size of the epiparietal differs from the ep 1 on ROM 73832, the incipient nature and the location of these epiparietals on the holotype and ROM 73832 suggests that they are homologous. Other parietals exhibit the presence of a variably sized epiparietal (ep 1) medial to the enlarged pachyostotic hook (ep 2) (see below for detailed description of WDC-DJR-002, ROM 73837 [Fig. 3.6, 3.7] and TMP 2002.069.0006).

The smaller pachyostotic process (ep 3) and the round triangular-shaped epiparietal (ep 4) are imbricated (Fig. 2.4). The pattern of imbrication indicates that the holotype preserves the left side of the frill, instead of the right side as Ryan et al. (2010) originally described. According to the re-orientation, the large pachyostotic hook (ep 2) slightly flexes ventrally at its base and has a distinct margin of the overgrowth on the ramus ventrally, which is similar to the condition of P1 and 2 of

https://doi.org/10.1017/jpa.2017.62 Published online by Cambridge University Press

Coronosaurus brinkmani parietals from the Milk River Ridge Reservoir bonebed (Ryan and Russell, 2005).

The lateral parietal ramus of WDC-DJR-001 has a wide gap (96.3 mm) between the squamosal contact and its anteriormost fused epiparietal (ep 4), which is unusual in centrosaurines. However, ROM 73834, which lacks this gap, has an epiparietal very close to the squamosal contact. The corresponding area of the holotype shows an open, asymmetrical, interdigiting suture on the lateral surface (Fig. 2.4), indicative of the prior presence of an unfused epiparietal (ep 5) that was lost post-mortem.

TMP 2002.069.0005 (Fig. 2.7, 2.8).—TMP 2002.069.0005 is composed of a right lateral ramus with a large pachyostotic ep 2, a lobe-like ep 3, and an undulating lateral surface representing the locus for unattached ep 4. The ep 3 and the ep 4 loci are imbricated. The ep 2 of this specimen differs in the lack of overgrowth at the base on the ventral side of the parietal ramus. The ep 3 is also smaller than that of WDC-DJR-001, but the morphology of this epiparietal is more similar to the anteriorly curved ep 3 on WDC-DJR-001 than to an unmodified epiparietal.

WDC-DJR-002 (paratype; Fig. 2.5, 2.6).—WDC-DJR-002 is a right half of the posterior ramus of the parietal. There is a large, laterally oriented, pachyostotic hook, which is comparable to ep 2 on WDC-DJR-001 and TMP 2002.069.0005. The ventral overgrowth of the ep 2 does not appear on this specimen, similar to TMP 2002.069.0005, but unlike WDC-DJR-001 and ROM 73837. Medial to the ep 2, this specimen has a lateral edge of the ep 1 on the posterior margin of the posterior ramus. Lateral to the ep 2, there is a partially preserved undulating surface representing a locus for ep 3, but the morphology of this ep 3 cannot be inferred due to the broken nature of the specimen.

FPDM-V-10 (not figured).—This specimen is a composite skeleton composed of the cranial and postcranial material from the Mansfield bonebed. Since the bonebed material was thought to represent a chasmosaurine, the frill reconstruction is incorrect. Three original frill specimens (not figured), including one partial midline ramus, one partial right ramus, and one partial left lateral ramus, are incorporated into the frill. The midline ramus has long-grained bone texture and a thin posterior margin (22.7 mm), suggesting this specimen is derived from a juvenile individual. There are three bumps along the dorsal midline, and the cross-section is triangular, as in centrosaurines. From posterior to anterior, the right lateral parietal ramus preserves a partial lobe-shaped epiparietal and two unmodified triangular epiparietals. The morphology and arrangement of the epiparietals on this specimen are congruent with the morphology of the ep 3-5 of other Mansfield bonebed parietal specimens (WDC-DJR-001 and TMP 2002.069.0005). The less complete left ramus has two unmodified, triangular epiparietals that likely represent ep 4 and ep 5.

ROM 77214 (not figured).—This specimen is a lateral bar of a right parietal preserving the squamosal contact, three epiparietals, and another epimarginal locus. This parietal ramus exhibits long-grained bone textures on both ventral and dorsal surfaces, suggesting it represents a relatively young individual. The anterolateral half of the pachyostotic ep 2 epiparietal locus is preserved. It is thickened (28.5 mm) compared to the lateral ramus (17.7 mm, measured lateral to the base of the ep 2) and protruding by at least ~60 mm from the lateral margin of the ramus (the tip of the epiparietal is slightly damaged). As indicated by the bone surface texture, we refer this epiparietal to an undeveloped ep 2. The ep 3 is a low (32.3 mm), broad-based (103.6 mm), and rounded epiparietal. This ep 3 is not pachyostotic, and its tip is not projecting anterolaterally, unlike the ep 3 of WDC-DJR-001. The ep 4 is low and triangular-shaped, and fused to the ramus. Ep 3 and 4 are imbricated. Anterolateral to the ep 3, the lateral margin of the ramus has a rugose texture continuing to the squamosal contact, suggesting this area represents an open suture for either a distinct ep 5 or an epiparietosquamosal. Although the epiparietals are not fully developed, the configuration of the epiparietals on this specimen is congruent with other parietals described above.

Squamosal.—None of the available squamosals are complete, but all show centrosaurine features. The preserved posterior flanges that form the lateral sides of frills are round rather than rectangular (ROM 73833, Fig. 5.4; TMP 2002.069.0003, Fig. 5.3), which is similar to taxa in the newly defined Eucentrosaura rather than basal centrosaurines (Maiorino et al., 2013). The maximum number of preserved episquamosals (or loci) on a single specimen is three (ROM 73833, Fig. 5.4; TMP 2002.069.0003, Fig 5.3). The profiles of the episquamosals are wide and low crescent-shaped (TMP 2002.069.0003), or sub-rectangular (ROM 73833) when viewed dorsally, except the anteriormost episquamosal on TMP 2002.069.0002, which is large, completely fused, and semicircular in outline. A ridge or a series of dorsal tori are often developed on the lateral side of centrosaurine squamosal, which are particularly prominent in early centrosaurines (Penkalski and Dodson, 1999; Evans and Ryan, 2015; Rivera-Sylva et al., 2016). These bumps are only weakly developed on TMP 2002.069.0002 (Fig. 5.1, 5.2), except for a larger eminence preserved on the anterodorsal part of the squamosal near the broken postorbital contact. The shape of the parietal contact of the squamosal is uncertain because this region is only preserved on the pathological WDC-DJR-017 (Ryan, 2007), however, the convex squamosal contacts of the parietals (e.g., ROM 73834) indicate that the squamosal has the typical centrosaurine concave parietal contact.

TMP 2002.069.0002 (Fig. 5.1, 5.2).—TMP 2002.069.0002 is a partial left squamosal. The anterior part is relatively intact and the jugal contact is almost completely preserved on the ventral side of the lateral surface, although the postorbital contact is damaged. Most of the posterior flange is missing except for the posteroventral corner, therefore the overall shape of the flange cannot be assessed. The corner is represented by a large, completely fused semicircular episquamosal. A ridge associated with a series of bumps is weakly developed on the dorsal side of the squamosal, except for a more prominent bump preserved on the anterodorsal part of the squamosal near the broken postorbital contact. The jugal notch is deeply embayed compared to the dorsal margin of lateral temporal fenestra.

TMP 2002.069.0003 (Fig. 5.3).—This specimen is a partial right squamosal lacking the anterior portion and the dorsal margin of the posterior flange. Three crescentic episquamosals are preserved and two of them are intact. Both of them are wide (97.1 and 110 mm for anteroventral and posterodorsal ones, respectively) and low when viewed dorsally.

https://doi.org/10.1017/jpa.2017.62 Published online by Cambridge University Press

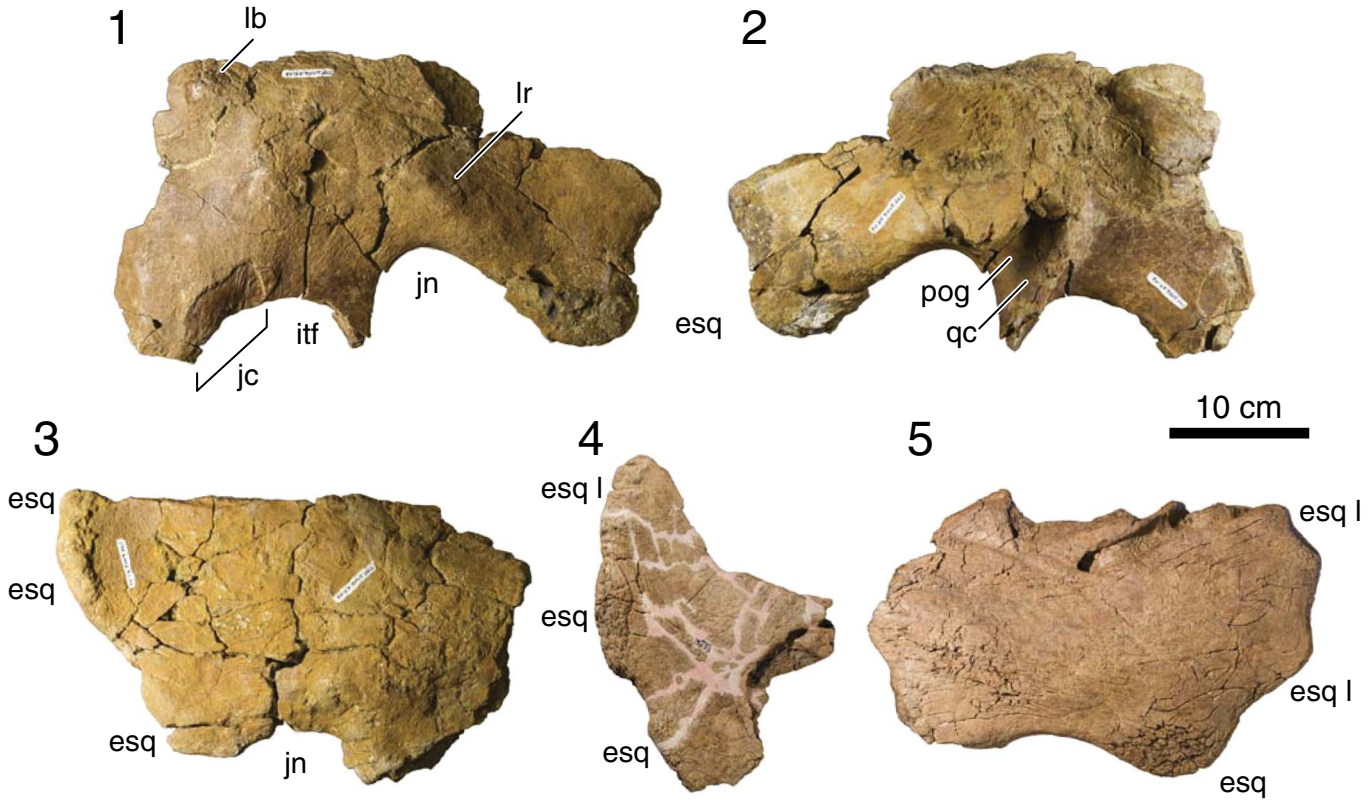

Figure 5. Squamosals from the Mansfield bonebed: (**1**) lateral and (**2**) medial views of TMP 2002.069.0002; (**3**) lateral view of TMP 2002.069.0003; (**4**) lateral view of ROM 73833; (**5**) lateral view of WDC-DJR-017. Abbreviations: esq, episquamosal; esql episquamosal locus; itf, infratemporal fenestra; jn, jugal notch; jc, jugal contact; lb, lateral bump; lr, lateral ridge; pog, paroccipital groove; qc, quadrate contact.

ROM 73833 (Fig. 5.4).—This specimen only preserves the posterior margin of the posterior flange with two episquamosals and an open, interdigitating suture at an episquamosal locus posterior to the two. The two episquamosals are wide (64.3 and 82.6 mm for anterior and posterior ones, respectively) and more rectangular than those of TMP 2002.069.0003. The inferred outline of the posterior flange is rounded, similar to TMP 2002.069.0003.

WDC-DJR-017 (Fig. 5.5).—This specimen is a partial left squamosal with a pathologically modified parietal contact (Ryan, 2007). There is an open suture for an episquamosal or epimarginal at the posterodorsal corner of the posterior flange. Two episquamosal loci are anterior to the open suture. The two preserved episquamosals are present completely fused and lack any evidence of their original sutural contact. A notch in the posterolateral squamosal margin represents the locus for an unfused epimarginal that straddled the parieto-squamosal suture.

Postorbital.—Several well-preserved postorbital horncores have been recovered from the Mansfield bonebed (Fig. 6). These span a large ontogenetic range of horncore morphology from small, triangular, centrosaurine-like horncores, to elongated and robust chasmosaurine-like horncores. The following detailed specimen descriptions are ordered by size, which presumably reflects the relative maturity of each individual at the time of death. The reported horncore lengths record the rectilinear length from the postorbital margin to the tip of the horncore.

TMP 2002.069.0010 (Fig. 6.1, 6.2, 6.12).—TMP 2002.069.0010 (Ryan, 2007; Fig. 10.4, 10.5) preserves a right postorbital with a complete horncore, but it is missing its posterior region. The short horncore (117.6 mm in length from the orbital margin to the tip of the horncore) is the smallest in the sample and the palpebral and frontal sutures are completely open (Fig. 6.1 and 6.2, respectively), suggesting it is from a juvenile individual. There is no evidence of a supracranial sinus system on this specimen. The horncore projects dorsally with slight anterolateral inclination (Fig. 6.1, 6.12). The gross morphology of the horncore is tall and pyramidal, which is similar to that of some juvenile centrosaurines (Ryan et al., 2001; Ryan and Russell, 2005). However, the round cross-sectional horncore base resembles those of juvenile

Figure 6. Postorbitals from the Mansfield bonebed; all of the specimens in this figure are represented by 3D models: (**1**) lateral and (**2**) medial views of TMP 2002.069.0010; (**3**) lateral and (**4**) medial views of ROM 73834; (**5**) ventral, (**6**) dorsal, (**7**) lateral, and (**8**) medial views of ROM 73831; (**9**) anterior, (**10**) right lateral views, and (**11**) the close-up of WDC-DJR-003; dotted line in (**11**) indicates shallow depression on the horncore; oblique views (direction is figured by arrows) of (**12**) TMP 2002.069.0010, (**13**) ROM 73834, and (**14**) ROM 73831, demonstrating ontogenetic change of postorbital horncores in *Medusaceratops lokii*. Abbreviations: aob, antorbital buttress; f, frontal; fc, frontal contact; ff, frontal fontanelle; lsc, laterosphenoid contact; o, orbit; pc, palpebral contact; poh, postorbital horncore; rp, resorption pit; scs, supracranial sinus.

https://doi.org/10.1017/jpa.2017.62 Published online by Cambridge University Press

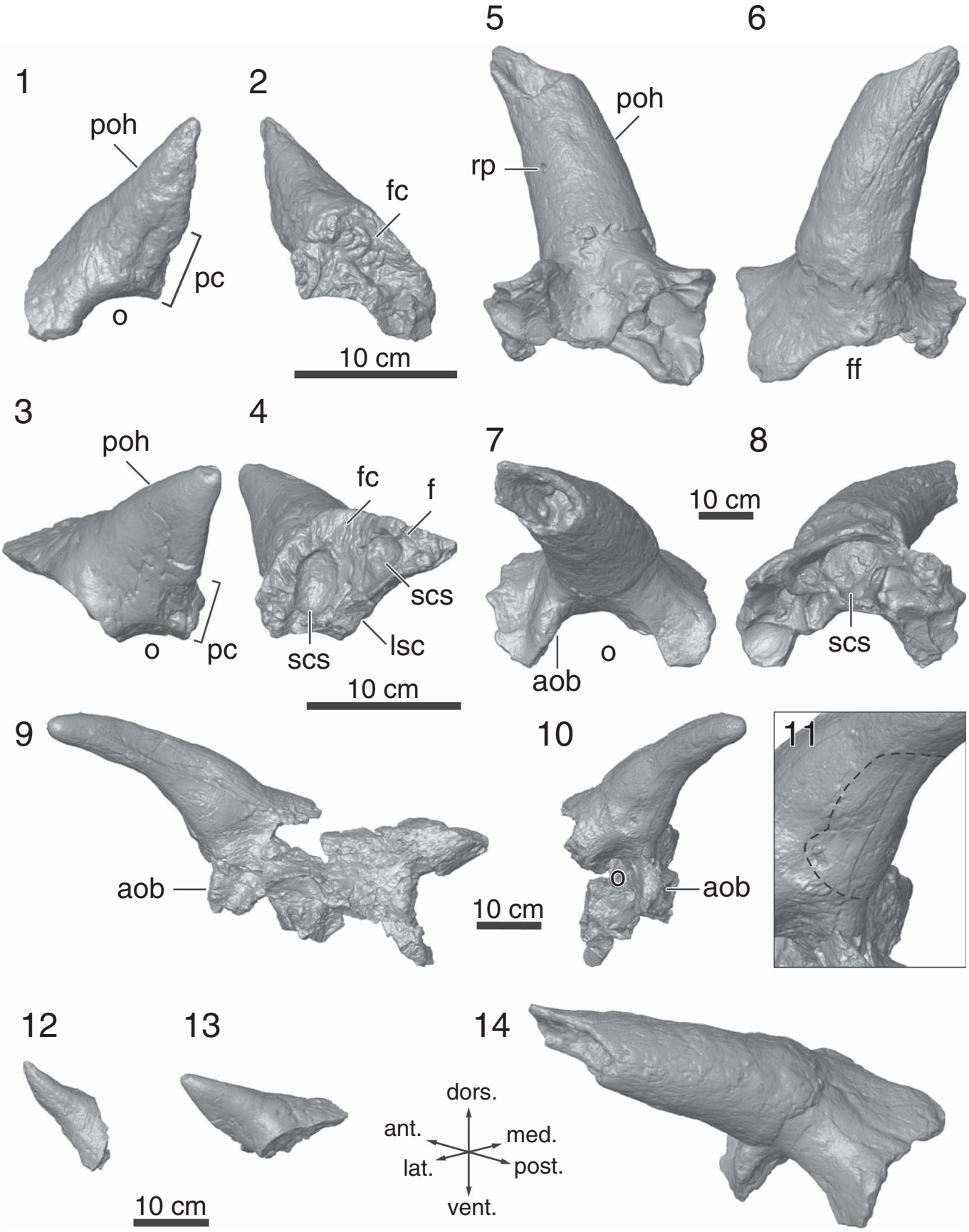

https://doi.org/10.1017/jpa.2017.62 Published online by Cambridge University Press

chasmosaurines (Currie et al., 2016; Lehman et al., 2016) and *Zuniceratops* (Wolfe et al., 2010).

ROM 73834 (Fig. 6.3, 6.4, 6.13).—This specimen only preserves the horncore portion of a right postorbital. The palpebral contact is completely open (Fig. 6.4). The frontal suture is only open anterior to the horncore and the frontal is indistinguishably fused posteriorly. The supracranial sinus system is represented by two depressions on the medioventral surface of the specimen (Fig. 6.4) that do not invade the shaft of the horncore, as is the typical condition for Centrosaurini (Farke, 2010). The length of the horncore (139.7 mm) is ~20% longer than that of TMP 2002.069.0010 (Fig. 6.12). The cross section of the horncore is more flattened and triangular than that of TMP 2002.069.0010, with its flat surface projecting posterolaterally rather than laterally as for juvenile *Centrosaurus apertus* (Ryan et al., 2001, figs. 10C–10F) and *Coronosaurus brinkmani* (Ryan and Russell, 2005).

WDC-DJR-003 (Fig. 6.9–6.11).—This specimen preserves the supraorbital region (fused lacrimals, palpebrals, postorbitals, and frontals) with the almost complete right (the tip is reconstructed in the figure) and incomplete left horncores. The preserved horncore length is 296 mm with a basal circumference of 383 mm. Unlike TMP 2002.069.0010 and ROM 73834, the cross-section of these horncores is circular (although they have been slightly distorted taphonomically). The horncore is strongly laterally oriented, but this is exaggerated due to the deformation (Fig. 6.9, 6.10). The basal overgrowth of the contact surface for the keratinous sheath, which is prominent on ROM 73831, is only poorly developed on the dorsoposterior two-thirds of the basal circumference of this specimen. A unique shallow, broad depression occurs on the anterior and ventral side of the horncore base, which is different from small round deep pit on the ROM 73831 (Fig. 6.11).

The frontal fontanelle margin is intact anteriorly, and it seems to have been open at the time of death. The supracranial sinus system is restricted to the base of the horncores. The antorbital buttress is swollen, making an oval-shaped eminence in lateral view (Fig. 6.10).

ROM 73831 (Fig. 6.5–6.8, 6.14).—ROM 73831 is a large (the basal circumference is 500 mm) left postorbital fused with its complementary lacrimal, palpebral, and frontal. The massive horncore is similar to those of *Albertaceratops*. The anterior region of the orbital rim is thickened, creating a prominent antorbital buttress (Fig. 6.7). The medial margin of the frontal does not reach the midline, indicating an open frontal fontanelle. The supracranial sinus (Fig. 6.8) partially invades the horncore at its base, similar to that seen in WDC-DJR-003. The tip of the horncore is broken and missing, and therefore the total length of the horncore is unknown, but the circumference of the horncore at its base is large (500 mm) and comparable to the largest horncore size of the non-Triceratopsini chasmosaurines (510 mm in *Pentaceratops sternbergii*, Wiman, 1930; Fig. 7; Table S2). The cross-section of the horncore is circular throughout the entirety of its preserved length. The horncore has a strong lateral inclination (~80° from the sagittal plane in the dorsal and ventral view), with only a limited projection dorsally (~20° from the horizontal plane in the anterior and posterior view). The horncore also has a slight curvature in dorsal and ventral views, but far less than that of *Nasutoceratops* (Sampson et al., 2013; Lund et al., 2016b).

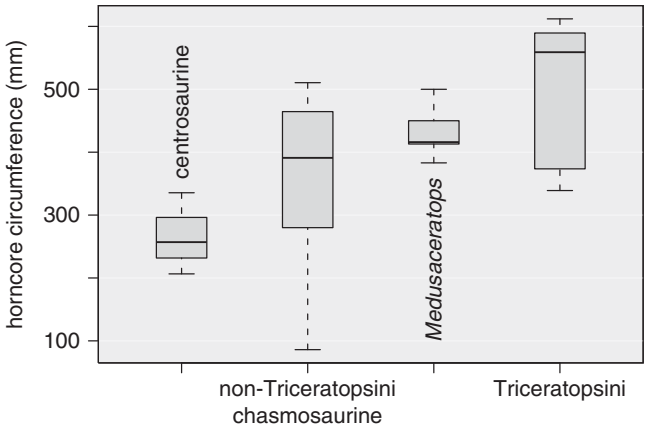

Figure 7. Comparison of postorbital horncore basal circumference between *Medusaceratops*, Centrosaurinae, non-Triceratopsini Chasmosaurinae, and Triceratopsini. In the box plots, mean values are represented by lines in the boxes, lower and upper bounds of the boxes represent the first and third quartiles, and the ends of the dashed lines indicate minimum and maximum values of the data. Data used for this plot are provided in Table S2.

The horncore has an unusual overgrowth that creates the step at the base of the horncore (Fig. 6.5, 6.6), which is also seen in the postorbital horncores of *Albertaceratops nesmoi* Ryan, 2007. *Spiclypeus shipporum* Mallon et al., 2016 also has a step at the base of the right postorbital horncore, but the step is restricted to the posterior side of the horncore, and it appears to be formed by extensive pitting rather than overgrowth. The holotype horncores of '*Ceratops montanus*' (Marsh, 1888) from the Judith River Formation (Mallon et al., 2016) do not have this overgrowth. On the ventral side of the horncore, there is a round foramen that is suggestive of resorption (Fig. 6.5), which is known to occur in postorbital horncores of various eucentrosauran centrosaurines, such as *Coronosaurus* (Ryan and Russell, 2005), *Spinops* (Farke et al., 2011), *Centrosaurus* (Ryan et al., 2001; Tanke and Farke, 2006), *Styracosaurus* (Ryan et al., 2007), and *Einiosaurus* (Sampson, 1995), but not in non-Eucentrosaura centrosaurines.

Nasal.—The nasals of *Medusaceratops* lack a distinct vertical horncore but instead have ornamentation that is in the form of a low, elongate, rugose ridge. No new nasal material can be added to the sample described by Ryan (2007). We re-examined the available nasals from the bonebed, but have no significant morphological observations beyond those in Ryan (2007); we therefore direct the reader to the appropriate section of that publication.

Osteohistological ontogenetic assessment

In order to assess the potential that the material from the Mansfield bonebed represents the full ontogenetic sequence of this taxon, the distal end of a left tibia from the bonebed (ROM 67873) was histologically sampled at its minimum diaphyseal circumference. This specimen represents one of the largest individuals among the bonebed material (minimum circumference = 300 mm). The mid-diaphysis is very robust and the lateral half of the distal end, where the calcaneum articulated, is extended distally compared to the medial half, which is characteristic of ceratopsids. Although it cannot be unequivocally referred to *Medusaceratops*, it is

https://doi.org/10.1017/jpa.2017.62 Published online by Cambridge University Press

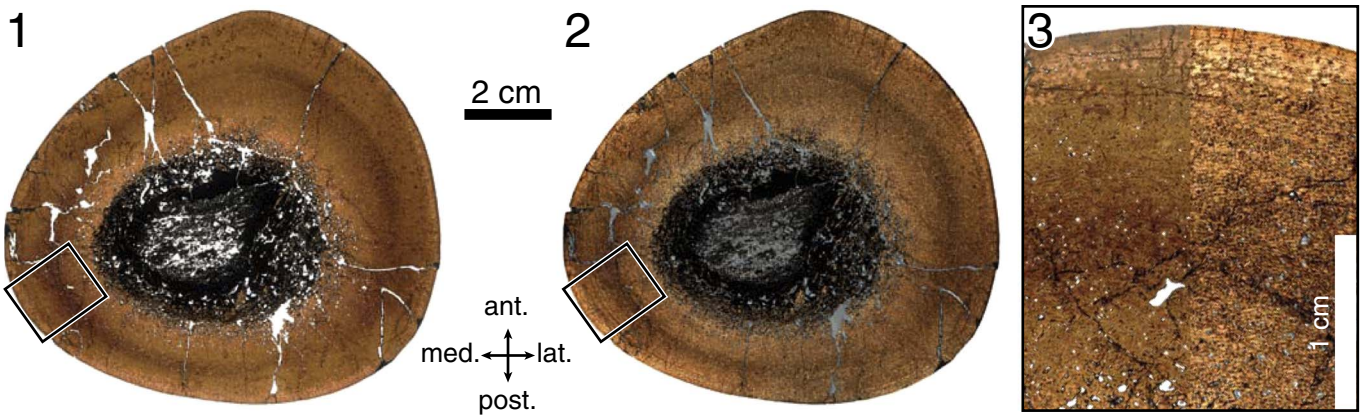

Figure 8. Thin-section photographs of mid diaphyseal cross-section of a tibia from the Mansfield bonebed (ROM 67873). Whole cross section images under (**1**) plane polarized and (**2**) cross-polarized light; (**3**) close-up images under plane polarized (left half) and cross-polarized light (right half).

unequivocally ceratopsid, and, given that no other ceratopsids can be confirmed from the locality, we infer that this specimen represents the tibia of *Medusaceratops*.

The mid-diaphyseal thin section of ROM 67873 is mainly composed of densely vascularized secondary bone (Fig. 8). A lenticular medullary cavity (~3 cm × 2.5 cm) is decentered posteriorly. A 0.5–1 cm layer of trabecular bone consistently surrounds the medullary cavity, except on the lateral side where the trabecular bone spans 3 cm. The cortical bone is distributed relatively consistently on the posterior half of the shaft (2 cm), but gradually thickens towards the anteriormost part where cortical bone thickness reaches ~3 cm. The cortical bone is composed of heavily remodeled Haversian bone with occasional Volkmann's canals. Therefore, primary bone tissue is severely obliterated, except in a thin peripheral region ~5 mm from the outer periosteal margin. The primary bone tissue along the outer periphery of the bone is comprised of poorly vascularized, parallel-fibered bone tissue with multiple growth lines that likely represent closely packed lines of arrested growth (LAGs), although any given growth mark cannot be traced around the entire periphery of the bone. Spacing between these growth lines rapidly narrows towards the outer periosteal margin, and forms an external fundamental system (EFS; Fig. 8.3). Extensive remodeling, parallel-fibered bone, and the presence of an EFS indicate that this individual had reached its asymptotic body size. This indicates that the largest individuals in the Mansfield bonebed were likely mature individuals, and allows comparisons of body size with other later ceratopsids (see Discussion).

Phylogenetic analysis

Medusaceratops could be coded for 64 out of 101 characters in the phylogenetic analysis (Supplemental data). The analysis recovered 630 most parsimonious trees, each with 181 steps. The Consistency Index and Retention Index of each most parsimonious tree is 0.624 and 0.791, respectively. In the strict consensus tree (Fig. 9), *Medusaceratops lokii* is supported by three autapomorphies (character 59[2], elongate flattened ep 2; character 60[1], laterally curved ep 2; and, character 62[1] laterally curved ep 3). *Medusaceratops* is nested within Centrosaurinae with four unambiguous synapomorphies (character 1[0], a rostral with short dorsal and ventral processes; character 2[1], a semicircular premaxillary septum; character 8[1], caudoventral expansion of a premaxilla, and character 51[1], a relatively wide parietal midline bar) and one ambiguous character (character 3[1], the septum composed of premaxilla and nasal).

Medusaceratops is recovered in a polytomy with *Albertaceratops*, *Wendiceratops* + *Sinoceratops*, and the newly defined clade Eucentrosaura. In our analysis, this new clade includes Centrosaurini (sensu Maiorino et al., 2015 and Ryan et al., 2017; *Rubeosaurus*, *Styracosaurus*, *Spinops*, *Centrosaurus*, *Coronosaurus*), *Einiosaurus*, and members of Pachyrostora with nasal bosses (sensu Fiorillo and Tykoski, 2012). Eucentrosaura does not include *Xenoceratops, Wendiceratops*, or *Sinoceratops*, unlike Sampson et al. (2013) and Lund et al. (2016a, 2016b), where these taxa were recovered in Pachyrhinosaurini. The members of Eucentrosaurua here have five synapomorphies: 17[1], maxillary tooth row at the same level as the rostral edentulous portion of the maxilla; 20 [1], presence of a distinct nasal horncore; 28[0], short postorbital horncore; 66[1], presence of ep 6; 68[1], presence of ep 7. *Xenoceratops* is recovered as the sister taxon to the least inclusive clade containing *Medusaceratops* and Pachyrostra in the strict consensus tree. The overall morphology of the strict consensus tree is similar to that of Evans and Ryan (2015) and Ryan et al. (Ryan et al., 2017), except for the loss of resolution in the strict consensus tree within the Centrosaurini.

The strict consensus topology recovered in this analysis is generally weakly supported, as is typical of most recent centrosaurine phylogenetic analyses (e.g., Evans and Ryan, 2015). Within Ceratopsidae, the Bremer Decay Index is only high (>2) at the bases of Chasmosaurinae, Centrosaurinae, Pachyrhinosaurini, and the genus *Pachyrhinosaurus*, with most nodes within Centrosaurinae having a Bremer Decay value of 1. Bootstrap values shows similar patterns of relative support (Fig. 9).

The constrained analysis, in which *Medusaceratops lokii* is inferred to be a chasmosaurine, resulted in eight extra steps in the most parsimonious trees compared to the original analysis where it is recovered nested within Centrosaurinae.

https://doi.org/10.1017/jpa.2017.62 Published online by Cambridge University Press

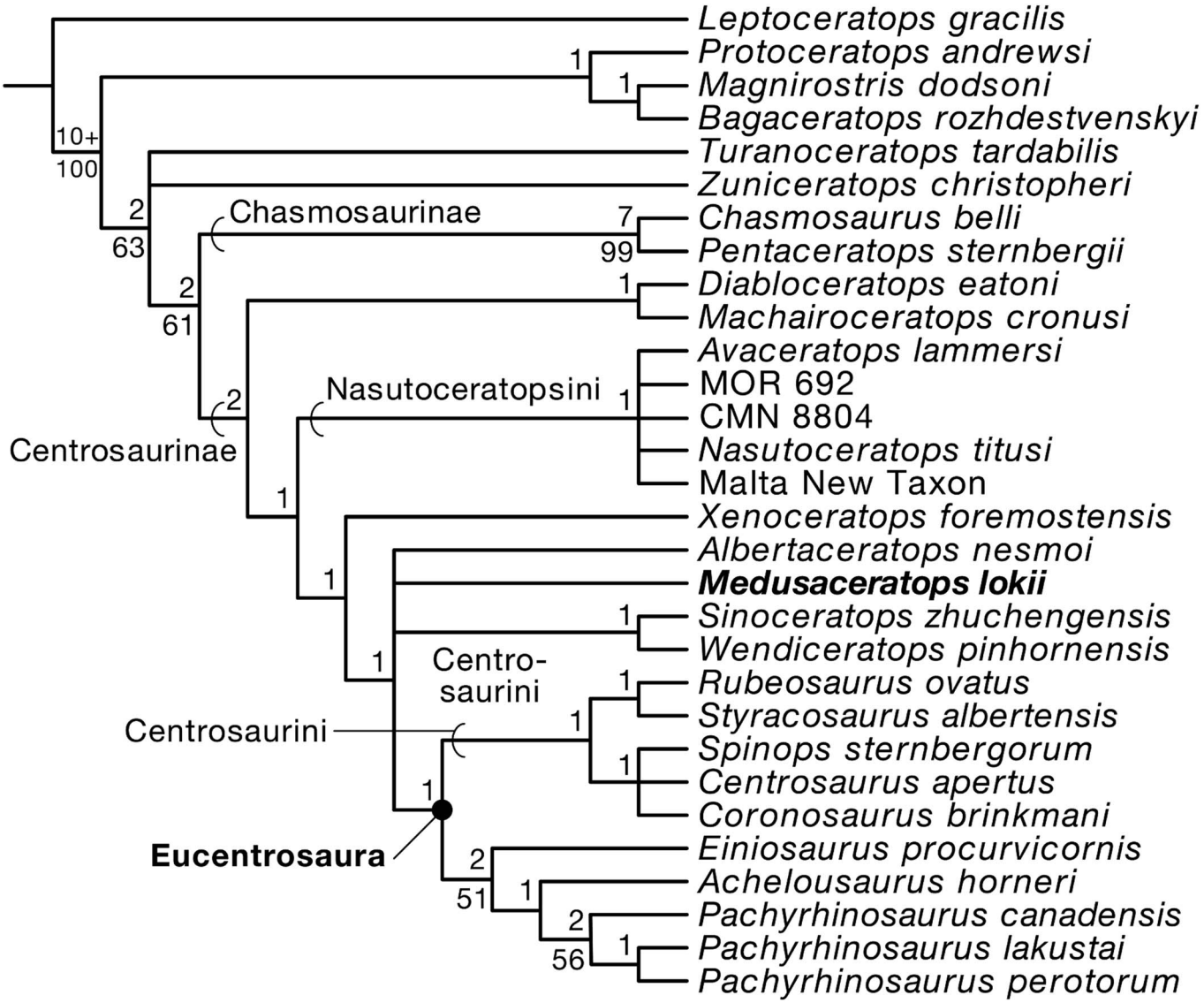

Figure 9. Strict consensus tree of the phylogenetic analysis in this paper. Numbers on nodes are decay indices (above) and bootstrap supports (below). Additional information available in supplemental data.

Discussion

The reassignment of *Medusaceratops* to Centrosaurinae resolves the unusual occurrence of pachyostotic frill ornamentation in the early chasmosaurines, to which it previously had been referred (Ryan, 2007), and supports the observation of Longrich (2013), who suggested that *Medusaceratops* was a member of Centrosaurinae based on the architecture of the parietal-squamosal contact.

In the original description of *Medusaceratops* (Ryan et al., 2010), the number of the epiparietals on the holotype and the paratype parietals was counted as three (Fig. 4.2). Because many chasmosaurines have three epiparietals on each side of the midline (Dodson et al., 2004), and all known centrosaurines have at least five epiparietals, *Medusaceratops* was described as a member of Chasmosaurinae (Ryan et al., 2010). However, it was an unusual member of this clade due to the presence of hypertrophied epiparietal hooks, which are otherwise typical of centrosaurines. Longrich (2013) argued that the utility of the number of epiparietals for distinguishing the two ceratopsid subfamilies is debatable, and cited the morphology of the parietosquamosal joint to argue for a centrosaurine affinity for *Medusaceratops*, but did not conclude if *Medusaceratops* was conspecific with *Albertaceratops*, or if it was a distinct centrosaurine species. The lack of a posterior midline ramus associated with either type specimen of *Medusaceratops* made it unclear up to that point whether the whole array of epiparietals was unknown for this taxon.

Description of the newly acquired material, including the first midline parietal ramus, and subsequent reexamination of the type specimens, provides new information that indicates *Medusaceratops* is a distinct species of centrosaurine ceratopsid. The holotype is now reinterpreted to have five epiparietals (Character 57[1]), a character changing the state at the base node of Centrosaurinae in the strict consensus tree. In addition, the new parietals exhibit diagnostic centrosaurine

https://doi.org/10.1017/jpa.2017.62 Published online by Cambridge University Press

traits, including a broad midline ramus on ROM 73832, imbricated epiparietals on ROM 73836 (also seen on the previously described specimens, WDC-DJR-001 and TMP 2002.069.0005), and a convex squamosal contact on ROM 73836 (also seen on WDC-DJR-001). The constrained analysis, in which *Medusaceratops lokii* is inferred to be a chasmosaurine, resulted in a hypothesis of eight extra steps compared to the original analysis, strongly supporting *Medusaceratops* as a member of Centrosaurinae.

Our new reconstruction of the parietal ornamentation of *Medusaceratops* allows for more detailed comparison to *Albertaceratops* and other ceratopsids. *Medusaceratops* is most similar to *Xenoceratops* in terms of having a small dorsally projecting ep 1 and a large pachyostotic and laterally projecting ep 2; however, the ep 2 of *Xenoceratops* is straight in the two known specimens, unlike the strongly curved ep 2 of *Medusaceratops*. Although we assigned epiparietal numbers from the midline laterally, following the character coding methodology of Evans and Ryan (2015), the laterally oriented ep 2 of *Medusaceratops* is morphologically similar to the massive ep 1 of *Albertaceratops*. Therefore, it is possible that these two epiparietals could be homologous (i.e., the ep 1 is not developed in *Albertaceratops* as has been inferred for *Pachyrhinosaurus*), which is congruent with the interpretation of *Albertaceratops* parietal ornamentation in Farke et al. (2011), who assigned the large pachyostotic epiparietal of this taxon to ep 2. More work on the homology of ceratopsid frill ornamentation is needed to resolve these issues (e.g., Farke et al., 2011).

We also note that the ep 1 is expressed differently on ROM 73832, where it occurs on the dorsal surface of the parietal ramus medially and extends to the posterior surface laterally, than on the holotype, where it is so much smaller that it was not recognized as an epiparietal by Ryan et al. (2010). The basal centrosaurines *Wendiceratops* and *Xenoceratops* also exhibit a high degree of intraspecific plasticity in epiparietal size and morphology. For example, in the holotype of *Xenoceratops*, the morphology of ep 1 is asymmetrical. On the left side, it is dorsally curved and larger than on the right side, where it does not appear to curve dorsally. In *Wendiceratops*, the size of the lateral epiparietals varies considerably from the subadult specimen (TMP 2011.051.0019) compared to the holotype (TMP 2011.051.0009). Similarly, eucentrosaurans can display a large degree of intraspecific variability in mature size, shape, and symmetry of their most-prominent epiparietals. For example, the ep 1 of *Centrosaurus apertus* (e.g., AMNH 5239, Brown, 1914a; CMN 971, Frederickson and Tumarkin-Deratzian, 2014), *Styracosaurus albertensis* (Ryan et al., 2007, fig. 14B), and ep 3 of *Pachyrhinosaurus lakustai* Currie, Langston, and Tanke, 2007 (Currie et al., 2007, figs. 32, 33) exhibits considerable variation, but this clade is generally very conservative within the other epiparietals. Thus, it is possible that a high degree of plasticity across all epiparietals may be plesiomorphic for Centrosaurinae, with this variability being primarily limited to only the prominently modified, more medially positioned epiparietals in eucentrosaurans. A future quantitative study of intraspecific frill variability may lead to refinement of ceratopsid systematics and phylogenetics studies.

The large size of the thin-sectioned tibia and the postorbital horncores of *Medusaceratops* are notable for an early ceratopsid.

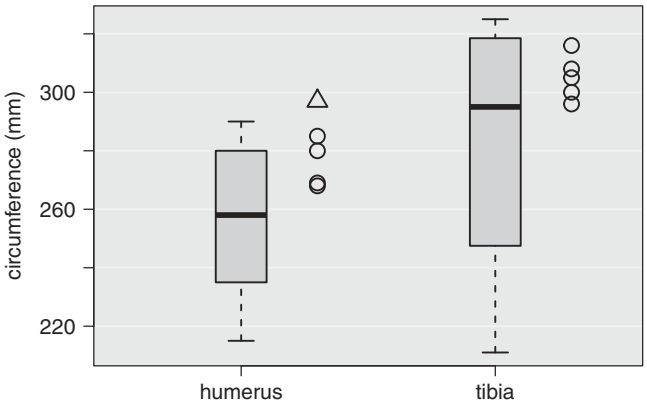

Figure 10. Comparison of humerus and tibia circumference of ceratopsids from the Belly River Group and the Judith River Formation. In the box plots, mean values are represented by lines in the boxes, lower and upper bounds of the boxes represent the first and third quartiles, and the ends of the dashed lines indicate minimum and maximum values of the data. Data used for this plot are provided in Table S3. Open circles and triangles represent *Medusaceratops* and *Wendiceratops*, respectively.

The size range of *Medusaceratops* limb elements, as well as the humeral size of the penecontemporaneous centrosaurine *Wendiceratops* (Evans and Ryan, 2015), are comparable to the late Campanian centrosaurines such as *Centrosaurus* and *Styracosaurus,* as well as the non-Triceratopsini chasmosaurines from the Belly River Group and correlative strata of the Judith River Formation (Fig. 10; Table S3). *Centrosaurus apertus* Lambe, 1904 and *Styracosaurus albertensis* have adult basal skull lengths that range in size from 666 mm to 786 mm (Table S3), with associated estimated body masses between 2,500 and 4,800 kg (body mass estimation based on sum of humerus and femur circumference using an interspecific limb scaling equation provided in Campione and Evans, 2012; Table S3). Earlier ceratopsids, notably the middle Campanian (~79 Ma) *Diabloceratops* (basal skull length = 620 mm; Kirkland and DeBlieux, 2010) and *Machairoceratops*, the holotype of which is interpreted as being approximately the same size as *Diabloceratops* (Lund et al., 2016a), are smaller than *Centrosaurus* and *Styracosaurus*. The large body size of *Medusaceratops* and *Wendiceratops* extends the fossil record of large-bodied ceratopsids into the middle Campanian and may have implications for the paleobiology of these taxa.

After examination of all available material, no unequivocal chasmosaurine bones, or diagnostic material from any other ceratopsid, could be identified in the Mansfield bonebed collections, suggesting that it represents a monodominant accumulation of a single centrosaurine taxon, *Medusaceratops*. The stratigraphic positions of the Mansfield *Medusaceratops* bonebed within the lower half of the Judith River Formation at Kennedy Coulee, Montana, the chronostratigraphically equivalent *Wendiceratops* bonebed from the lower Oldman Formation of Alberta (Evans and Ryan, 2015), and a low-density bonebed of *Xenoceratops* from the slightly chronostratigraphically older Foremost Formation (Ryan et al., 2012) mark some of the oldest occurrences of centrosaurine bonebeds. Monodominant centrosaurine bonebeds become more abundant in slightly higher stratigraphic units (e.g., *Coronosaurus brinkmani* from younger strata of the Oldman Formation; Ryan and Russell, 2005), and are common in the Dinosaur Park Formation and younger strata in Alberta,

https://doi.org/10.1017/jpa.2017.62 Published online by Cambridge University Press

Montana, and Alaska. The detailed taphonomic studies of the *Centrosaurus apertus* bonebeds in the Belly River Group indicate that these deposits represent mass death assemblages of massive herds of centrosaurs (Ryan et al., 2001; Eberth and Getty, 2005; Eberth et al., 2010; Chiba et al., 2015). To date, detailed taphonomic analyses have yet to be carried out on the *Medusaceratops* and *Wendiceratops* bonebeds, but such studies could lead to important insights into the palaeobiology of early ceratopsids. Previous taphonomic work on more derived taxa, and examples of basal neoceratopsian and *Zuniceratops* bonebeds (Hunt and Farke, 2010; Wolfe et al., 2010) suggest that large-scale gregarious behavior has deep evolutionary roots in Ceratopsia and may be plesiomorphic for Centrosaurinae.

Acknowledgments

We thank D. Brinkman, B. Strilisky, G. Housego, B. Bavington-Sanchez, T. Courtenay, and R. Russell for specimen access in Royal Tyrrell Museum of Palaeontology. A. Guyon and L. Shinkle provided specimen access in the Wyoming Dinosaur Center, and C. Levitt-Bussian for specimen access at the Natural History Museum of Utah. M. Shibata, T. Sekiya, T. Sonoda, S. Kawabe, H. Yukawa facilitated specimen access in the Fukui Prefectural Dinosaur Museum. We thank A. Dzindic (Canada Fossils Ltd.) for his care in preparing many of the specimens, and I. Morrison for preparation at the ROM, as well as J. Issa (Canada Fossils Ltd.) for specimen loans and facilitating specimen acquisition. We thank D. Trexler (Two Medicine Dinosaur Center) for providing the information on WDCB-MC-001. We are grateful to D. and L. Redding, and M. Goodwin (University of California Museum of Paleontology) for fieldwork logistics, and T. Cullen (University of Toronto) for assistance in the field. Thanks to K. Seymour and B. Iwama for logistical support at the ROM. We thank A. Farke for a constructive review, and K. Brink and D. Eberth (Royal Tyrrell Museum of Palaeontology) for discussions and editorial assistance.

The Dinosaur Research Institute for provided a travel grant to KFC to present this study at the Society of Vertebrate Paleontology annual meeting in 2016. The Louise Hawley Stone Charitable Trust and Royal Ontario Museum provided funding to acquire specimens for this project. DCE was supported by a Natural Sciences and Engineering Research Council of Canada Discovery Grant (NSERC Grant File Number: RGPIN 355845). Fieldwork associated with this research was supported by the Royal Ontario Museum Reproductions Fund and the ROM Collections & Research Fieldwork Fund. The Willi Henning Society provided access to TNT.

Accessibility of supplemental data

Data available from the Dryad Digital Repository: http://doi.org/10.5061/dryad.8h067

Supplemental data include the following:

Text S1. List of the Mansfield bonebed specimens used for character coding.

Table S1. Specimen list of the Mansfield bonebed material housed in museum collections.

Table S2. Compiled postorbital horncore measurements of Centrosaurinae, non-Triceratopsini Chasmosaurinae, and Triceratopsini.

Table S3. Compiled humerus and tibia circumference mea surements of ceratopsids from Belly River Group and Judith River Formation (Campanian).

Supplemental data 1. Data matrix used in phylogenetic analysis in this study (TNT file).

Supplemental data 2. 3D data of a *Medusaceratops* parietal (ROM 73832, STL file).

Supplemental data 3. 3D data of a *Medusaceratops* parietal (ROM 73837, STL file).

Supplemental data 4. 3D data of a *Medusaceratops* postorbital (TMP 2002.069.0010, STL file).

Supplemental data 5. 3D data of a *Medusaceratops* postorbital (ROM 73834, STL file).

Supplemental data 6. 3D data of a *Medusaceratops* postorbital (ROM 73831, STL file).

Supplemental data 7. 3D data of a *Medusaceratops* postorbital (WDC-DJR-003, STL file).

Supplemental data 8. Thin section photograph of mid diaphy seal cross-section of a *Medusaceratops* tibia (ROM 67873) with plane polarized light (JPG file).

Supplemental data 9. Thin section photograph of mid diaphy seal cross-section of a *Medusaceratops* tibia (ROM 67873) with cross polarized light (JPG file).

References

Brinkman, D.B., Russell, A.P., Eberth, D.A., and Peng, J., 2004, Vertebrate palaeocommunities of the lower Judith River Group (Campanian) of southeastern Alberta, Canada, as interpreted from vertebrate microfossil assemblages: Palaeogeography, Palaeoclimatology, Palaeoecology, v. 213, p. 295–313.

Brown, B., 1914a, A complete skull of *Monoclonius*, from the Belly River Cretaceous of Alberta: Bulletin of American Museum of Natural History, v. 33, p. 549–558.

Brown, B., 1914b, *Leptoceratops*, a new genus of Ceratopsia from the Edmonton Cretaceous of Alberta: Bulletin of the American Museum of Natural History, v. 33, p. 567–580.

Brown, C.M., Russell, A.P., and Ryan, M.J., 2009, Pattern and transition of surficial bone texture of the centrosaurine frill and their ontogenetic and taxonomic implications: Journal of Vertebrate Paleontology, v. 29, p. 132–141.

Campbell, J.A., Ryan, M.J., Holmes, R.B., and Schröder-Adams, C.J., 2016, A re-evaluation of the chasmosaurine ceratopsid genus *Chasmosaurus* (Dinosauria: Ornithischia) from the Upper Cretaceous (Campanian) Dinosaur Park Formation of western Canada: PLoS ONE, v. 11, e0145805, https://doi.org/10.1371/journal.pone.0145805.

Campione, N.E., and Evans, D.C., 2012, A universal scaling relationship between body mass and proximal limb bone dimensions in quadrupedal terrestrial tetrapods: BMC Biology, 10:60. doi: 10.1186/1741-7007-10-60.

Chiba, K., Ryan, M.J., Braman, D. R., Eberth, D.A., Scott, E.E., Brown, C.M., Kobayashi, Y., and Evans, D.C., 2015, Taphonomy of a monodominant *Centrosaurus apertus* (Dinosauria: Ceratopsia) bonebed from the upper Oldman Formation of southeastern Alberta: Palaios, v. 30, p. 655–667.

Cullen, T.M., Fanti, F., Capobianco, C., Ryan, M.J., and Evans, D.C., 2016, A vertebrate microsite from a marine-terrestrial transition in the Foremost Formation (Campanian) of Alberta, Canada, and the use of faunal assemblage data as a paleoenvironmental indicator: Palaeogeography, Palaeoclimatology, Palaeoecology, v. 444, p. 101–114.

Currie, P.J., Langston, W., and Tanke, D.H., 2008, A New Horned Dinosaur From an Upper Cretaceous Bone Bed in Alberta: Ottawa, Ontario, NRC Research Press, 144 p.

Currie, P.J., Holmes, R.B., Ryan, M.J., and Coy, C., 2016, A juvenile chasmosaurine ceratopsid (Dinosauria, Ornithischia) from the Dinosaur Park Formation, Alberta, Canada: Journal of Vertebrate Paleontology, v. 36, e1048348. https://doi.org/10.1080/02724634.2015.1048348.

Dodson, P., Forster, C.A., and Sampson, S.D., 2004, Ceratopsidae, *in* Weishampel, D.B., Dodson, P., and Osmólska, H., eds., The Dinosauria: Berkeley, University of California Press, p. 494–513.
Eberth, D.A., 2015, Origins of dinosaur bonebeds in the Cretaceous of Alberta, Canada: Canadian Journal of Earth Sciences, v. 52, p. 655–681.
Eberth, D.A., and Getty, M.A., 2005, Ceratopsian bonebeds: occurrence, origins, and significance, *in* Currie, P.J., Koppelhus, and E.B., eds., Dinosaur Provincial Park: A Spectacular Ancient Ecosystem Revealed: Bloomington, Indiana, Indiana University Press, p. 501–536.
Eberth, D.A., and Hamblin., A.P., 1993, Tectonic, stratigraphic, and sedimentologic significance of a regional discontinuity in the upper Judith River Group (Belly River wedge) of southern Alberta, Saskatchewan, and northern Montana: Canadian Journal of Earth Sciences, v. 30, p. 174–200.
Eberth, D.A., Brinkman, D.B., and Barkas, V., 2010, A centrosaurine megabonebed from the Upper Cretaceous of southern Alberta: implications for behavior and death events, *in* Ryan, M.J., Chinnery-Allgeier, B.J., and Eberth, D.A., eds., New Perspectives on Horned Dinosaurs: The Royal Tyrrell Museum Ceratopsian Symposium: Bloomington, Indiana, Indiana University Press, p. 495–508.
Evans, D.C., and Ryan, M.J., 2015, Cranial anatomy of *Wendiceratops pinhornensis* gen. et sp. nov., a centrosaurine ceratopsid (Dinosauria: Ornithischia) from the Oldman Formation (Campanian), Alberta, Canada, and the evolution of ceratopsid nasal ornamentation: PLoS ONE, v. 10, e0130007. https://doi.org/10.1371/journal.pone.0130007.
Farke, A.A., 2010, Evolution, homology, and function of the supracranial sinuses in ceratopsian dinosaurs: Journal of Vertebrate Paleontology, v. 30, p. 1486–1500.
Farke, A.A., Ryan, M.J., Barrett, P.M., Tanke, D.H., Braman, D.R., Loewen, M.A., and Graham, M.R., 2011, A new centrosaurine from the Late Cretaceous of Alberta, Canada, and the evolution of parietal ornamentation in horned dinosaurs: Acta Palaeontologica Polonica, v. 56, p. 691–702.
Fiorillo, A.R., and Tykoski, R.S., 2012, A new Maastrichtian species of the centrosaurine ceratopsid *Pachyrhinosaurus* from the North Slope of Alaska: Acta Palaeontologica Polonica, v. 57, p. 561–573. doi: 10.4202/app.2011.0033.
Fowler, D.W., 2016, A new correlation of the Cretaceous formations of the Western Interior of the United States, I: Santonian–Maastrichtian formations and dinosaur biostratigraphy: PeerJ Preprints, v. 4, e2554v1. https://doi.org/10.7287/peerj.preprints.2554v1
Frederickson, J.A., and Tumarkin-Deratzian, A.R., 2014, Craniofacial ontogeny in *Centrosaurus apertus*: PeerJ, v. 2, e252. https://doi.org/10.7717/peerj.252.
Freedman Fowler, E.A., and Horner., J.R., 2015, A new brachylophosaurin hadrosaur (Dinosauria: Ornithischia) with an intermediate nasal crest from the Campanian Judith River Formation of northcentral Montana: PLoS ONE, v. 10, e0141304. https://doi.org/10.1371/journal.pone.0141304
Goloboff, P.A., and Catalano, S.A., 2016, TNT version 1.5, including a full implementation of phylogenetic morphometrics: Cladistics, v. 32, p. 221–238. doi: 10.1111/cla.12160.
Goodwin, M.B., and Deino, A.L., 1989, The first radiometric ages from the Judith River Formation (Upper Cretaceous), Hill County, Montana: Canadian Journal of Earth Sciences, v. 26, p. 1384–1391.
Hunt, R.K., and Farke, A.A., 2010, Behavioral interpretations from ceratopsid bonebeds, *in* Ryan, M.J., Chinnery-Allgeier, B.J., and Eberth, D.A., eds., New Perspectives on Horned Dinosaurs: The Royal Tyrrell Museum Ceratopsian Symposium: Bloomington, Indiana, Indiana University Press, p. 447–455.
Kirkland, J.I., and DeBlieux, D.D., 2010, New basal centrosaurine ceratopsian skulls from the Wahweap Formation (middle Campanian), Grand Staircase—Escalante National Monument, southern Utah, *in* Ryan, M.J., Chinnery-Allgeier, B.J., and Eberth, D.A., eds., New Perspectives on Horned Dinosaurs: The Royal Tyrrell Museum Ceratopsian Symposium: Bloomington, Indiana, Indiana University Press, p. 117–140.
Lambe, L.M., 1904, On the squamosoparietal crest of two species of horned dinosaurs from the Cretaceous of Alberta: Ottawa Naturalist, v. 8, p. 81–84.
Lambe, L.M., 1913, A new genus and species of Ceratopsia from the Belly River Formation of Alberta: Ottawa Naturalist, v. 27, p. 109–116.
Lambe, L.M., 1915, On *Eoceratops Canadensis*, gen. nov., with remarks on other genera of Cretaceous horned dinosaurs: Canada Geological Survey, Museum Bulletin, v. 12, p. 1–49.
Lamm, E-.T., 2013, Preparation and sectioning of specimens, *in* Padian, K., and Lamm, E.-T.. Bone Histology of Fossil Tetrapods—Advancing Methods, Analysis, and Interpretation: Berkeley and Los Angeles, California, University of California Press, p. 55–160. doi: 10.1525/california/9780520273528.003.0004.
Lehman, T.M., Wick, S.L., and Barnes, K.R., 2016, New specimens of horned dinosaurs from the Aguja Formation of West Texas, and a revision of *Agujaceratops*: Journal of Systematic Palaeontology, v. 15, p. 641–674. http://dx.doi.org/10.1080/14772019.2016.1210683.
Loewen, M.A., Farke, A.A., Sampson, S.D., Getty, M.A., Lund, E.K., and O'Connor, P.M., 2013, Ceratopsid dinosaurs from the Grand Staircase of southern Utah, *in* Titus, A.L., and Loewen, M.A., eds., At the Top of the Grand Staircase: Bloomington, Indiana, Indiana University Press, p. 488–503.
Longrich, N.R., 2013, *Judiceratops tigris*, a new horned dinosaur from the Middle Campanian Judith River Formation of Montana: Bulletin of the Peabody Museum of Natural History, v. 54, p. 51–65.
Lund, E.K., O'Connor, P.M., Loewen, M.A., and Jinnah, Z.A., 2016a, A new centrosaurine ceratopsid, *Machairoceratops cronusi* gen et sp. nov., from the upper Sand Member of the Wahweap Formation (middle Campanian), southern Utah: PLoS ONE, v. 11, e0154403 doi: 10.1371/journal.pone.0154403.
Lund, E.K., Sampson, S.D., and Loewen, M.A., 2016b, *Nasutoceratops titusi* (Ornithischia, Ceratopsidae), a basal centrosaurine ceratopsid from the Kaiparowits Formation, southern Utah: Journal of Vertebrate Paleontology, v. 36, e1054936. https://doi.org/10.1080/02724634.2015.1054936.
Maiorino, L., Farke, A.A., Piras, P., Ryan, M.J., Terris, K.M., and Kotsakis, T., 2013, The evolution of squamosal shape in ceratopsid dinosaurs (Dinosauria, Ornithischia): Journal of Vertebrate Paleontology, v. 33, p. 1385–1393.
Maiorino, L., Farke, A.A., Kotsakis, T., Teresi, L., and Piras, P., 2015, Variation in the shape and mechanical performance of the lower jaws in ceratopsid dinosaurs (Ornithischia, Ceratopsia): Journal of Anatomy, v. 227, p. 631–646.
Mallon, J.C., Ott, C.J., Larson, P.L., Iuliano, E.M., and Evans, D.C., 2016, *Spiclypeus shipporum* gen. et sp. nov., a boldly audacious new chasmosaurine ceratopsid (Dinosauria: Ornithischia) from the Judith River Formation (Upper Cretaceous: Campanian) of Montana, USA: PLoS ONE, v. 11, e0154218. https://doi.org/10.1371/journal.pone.0154218.
Marsh, O.C., 1888, A new family of horned Dinosauria, from the Cretaceous: American Journal of Science, ser. 3, v. 36, p. 477–478.
Marsh, O. C., 1890, Additional Characters of the Ceratopsidae, with Notice of New Cretaceous Dinosaurs: American Journal of Science, ser. 3, v. 39, p. 418–426.
Ogunyomi, O., and Hills, L.V., 1977, Depositional environments, Foremost Formation (Late Cretaceous), Milk River area, southern Alberta: Bulletin of Canadian Petroleum Geology, v. 25, p. 929–968.
Owen, R., 1842, Report on British Fossil Reptiles. Part II: Report of the British Association for the Advancement of Science, Plymouth, v. 1841, p. 60–204.
Penkalski, P., and Dodson, P., 1999, The morphology and systematics of *Avaceratops*, a primitive horned dinosaur from the Judith River Formation (Late Campanian) of Montana, with the description of a second skull: Journal of Vertebrate Paleontology, v. 19, p. 692–711.
Ralrick, P. E., and Tanke, D.H., 2008, Comments on the quarry map and preliminary taphonomic observations of the *Pachyrhinosaurus* (Dinosauria: Ceratopsidae) bone bed at Pipestone Creek, Alberta, Canada, *in* Currie, P.J., Langston, W., Jr., and Tanke, D.H., eds., A New Horned Dinosaur From an Upper Cretaceous Bone Bed in Alberta: Ottawa, Ontario, NRC Research Press, p. 109–116.
Rivera-Sylva, H.E., Hedrick, B.P., and Dodson, P., 2016, A centrosaurine (Dinosauria: Ceratopsia) from the Aguja Formation (late Campanian) of northern Coahuila, Mexico: PLoS ONE, v. 11, e0150529.
Roberts, E.M., Sampson, S.D., Deino, A.L., Bowring, S.A., and Buchwaldt, R., 2013, The Kaiparowits Formation: a remarkable record of Late Cretaceous terrestrial environments, ecosystems, and evolution in western North America, *in* Titus, A.L., and Loewen, M.A., eds., At the Top of the Grand Staircase: Bloomington, Indiana, Indiana University Press, p. 85–106.
Rogers, R.R., Kidwell, S.M., Deino, A.L., Mitchell, J.P., Nelson, K., and Thole, J.T., 2016, Age, correlation, and lithostratigraphic revision of the Upper Cretaceous (Campanian) Judith River Formation in its type area (north-central Montana), with a comparison of low- and high-accommodation alluvial records: The Journal of Geology, v. 124, p. 99–135.
Ryan, M.J., 2007, A new basal centrosaurine ceratopsid from the Oldman Formation, southeastern Alberta: Journal of Paleontology, v. 81, p. 376–396.
Ryan, M.J., and Russell, A.P., 2005, A new centrosaurine ceratopsid from the Oldman Formation of Alberta and its implications for centrosaurine taxonomy and systematics: Canadian Journal of Earth Sciences, v. 42, p. 1369–1387.
Ryan, M.J., Russell, A.P., Eberth, D.A., and Currie, P.J., 2001, The taphonomy of a *Centrosaurus* (Ornithischia: Ceratopsidae) bone bed from the Dinosaur Park Formation (Upper Campanian), Alberta, Canada, with comments on cranial ontogeny: Palaios, v. 16, p. 482–506.
Ryan, M.J., Holmes, R., and Russell, A.P., 2007, A Revision of the Late Campanian centrosaurine ceratopsid genus *Styracosaurus* from the Western Interior of North America: Journal of Vertebrate Paleontology, v. 27, p. 944–962.
Ryan, M.J., Russell, A.P., and Hartman, S., 2010, A new chasmosaurine ceratopsid from the Judith River Formation, Montana, *in* Ryan, M.J.,

Chinnery-Allgeier, B.J., and Eberth, D.A., eds., New Perspectives on Horned Dinosaurs: The Royal Tyrrell Museum Ceratopsian Symposium: Bloomington, Indiana, Indiana University Press, p. 181–188.
Ryan, M.J., Evans, D.C., and Shepherd, K.M., 2012, A new ceratopsid from the Foremost Formation (middle Campanian) of Alberta: Canadian Journal of Earth Sciences, v. 49, p. 1251–1262.
Ryan, M.J., Evans, D.C., Currie, P.J., and Loewen, M.A., 2014, A new chasmosaurine from northern Laramidia expands frill disparity in ceratopsid dinosaurs: Naturwissenschaften, v. 101, p. 505–512.
Ryan, M.J., Holmes, R., Mallon, J., Loewen, M., and Evans, D.C., 2017, A basal ceratopsid (Centrosaurinae: Nasutoceratopsini) from the Oldman Formation (Campanian) of Alberta, Canada: Canadian Journal of Earth Sciences, v. 54, p. 1–14.
Sampson, S.D., 1995, Two new horned dinosaurs from the upper Cretaceous Two Medicine Formation of Montana; with a phylogenetic analysis of the Centrosaurinae (Ornithischia: Ceratopsidae): Journal of Vertebrate Paleontology, v. 15, p. 743–760. doi: 10.1080/02724634.1995.10011259.
Sampson, S.D., Ryan, M.J., and Tanke, D.H., 1997, Craniofacial ontogeny in centrosaurine dinosaurs (Ornithischia: Ceratopsidae): taxonomic and behavioral implications: Zoological Journal of the Linnean Society, v. 121, p. 293–337.
Sampson, S.D., Lund, E.K., Loewen, M.A., Farke, A.A., and Clayton, K.E., 2013, A remarkable short-snouted horned dinosaur from the Late Cretaceous (late Campanian) of southern Laramidia: Proceedings of the Royal Society B: Biological Sciences, v. 280, p. 1–7.
Seeley, H.G., 1887, On the classification of the fossil animals commonly named Dinosauria: Proceedings of the Royal Society of London, v. 43, p. 165–171.
Sereno, P.C., 1986, Phylogeny of the Bird-Hipped Dinosaurs (Order Ornithischia): National Geographic Research, v. 2, p. 234–256.
Tanke, D.H., and Farke, A.A., 2006, Bone resorption, bone lesions, and extracranial fenestrae in ceratopsid dinosaurs: a preliminary assessment, *in* Carpenter, K., ed., Horns and Beaks: Ceratopsian and Ornithopod Dinosaurs: Bloomington, Indiana, Indiana University Press, p. 319–347.
Wiman, C., 1930, Über Ceratopsia aus der Oberen Kreide in New Mexico: Nova Acta Regiae Societatis Scientiarum Upsaliensis Series, v. 7, p. 1–19.
Wolfe, D.G., Kirkland, J.I., Smith, D., Poole, K., Chinnery-Allgeier, B., and McDonald, A., 2010, *Zuniceratops christopheri*: the North American ceratopsid sister taxon reconstructed on the basis of new data, *in* Ryan, M.J., Chinnery-Allgeier, B.J., and Eberth, D.A., eds., New Perspectives on Horned Dinosaurs: The Royal Tyrrell Museum Ceratopsian Symposium: Bloomington, Indiana, Indiana University Press, p. 91–98.

Accepted 22 May 2017